UNCLASSIFIED
CONFIDENTIAL

NACA
RM-A51G27
48 c.1

NACA RM A51G27

CASE FILE COPY

GROUP 4
Downgraded at 3 year intervals; declassified after 12 years

NACA

RESEARCH MEMORANDUM

LONGITUDINAL FREQUENCY-RESPONSE CHARACTERISTICS OF A 35° SWEPT-WING AIRPLANE AS DETERMINED FROM FLIGHT MEASUREMENTS, INCLUDING A METHOD FOR THE EVALUATION OF TRANSFER FUNCTIONS

By William C. Triplett and G. Allan Smith

Ames Aeronautical Laboratory
Moffett Field, Calif.

Classification Changed to UNCLASSIFIED
Authority DOD DIR 5200.10
Date 11-5-64 By SCJackson

JPL LIBRARY
CALIFORNIA INSTITUTE OF TECHNOLOGY
OCT 2 1951

CLASSIFIED DOCUMENT

This document contains classified information affecting the National Defense of the United States within the meaning of the Espionage Act, USC 50:31 and 32. Its transmission or the revelation of its contents in any manner to an unauthorized person is prohibited by law.

Information so classified may be imparted only to persons in the military and naval services of the United States, appropriate civilian officers and employees of the Federal Government who have a legitimate interest therein, and to United States citizens of known loyalty and discretion who of necessity must be informed thereof.

NATIONAL ADVISORY COMMITTEE
FOR AERONAUTICS

WASHINGTON
September 19, 1951

CONFIDENTIAL
UNCLASSIFIED

UNCLASSIFIED
CONFIDENTIAL

TABLE OF CONTENTS

	Page
SUMMARY	1
INTRODUCTION	1
NOTATION	2
TEST EQUIPMENT	4
TEST PROCEDURE AND ANALYSIS	5
Flight Measurements	5
Frequency–Response Computations	6
Determination of Transfer Coefficients	8
Final Check	11
RESULTS AND DISCUSSION	11
Frequency–Response Curves	12
Transfer Functions	13
Elevator Effectiveness	14
Altitude Variations	14
ACCURACY	14
Nonlinearities	15
Instrumentation	16
Flight Technique	17
Data Reduction	17
CONCLUDING REMARKS	17
APPENDIX A	19

UNCLASSIFIED
CONFIDENTIAL

TABLE OF CONTENTS – Continued

Page

APPENDIX B 22

APPENDIX C 23

REFERENCES 25

FIGURES 27

NATIONAL ADVISORY COMMITTEE FOR AERONAUTICS

RESEARCH MEMORANDUM

LONGITUDINAL FREQUENCY-RESPONSE CHARACTERISTICS OF A 35° SWEPT-WING AIRPLANE AS DETERMINED FROM FLIGHT MEASUREMENTS, INCLUDING A METHOD FOR THE EVALUATION OF TRANSFER FUNCTIONS

By William C. Triplett and G. Allan Smith

SUMMARY

Longitudinal frequency-response characteristics of a 35° swept-wing airplane computed from flight measurements are presented herein. Pitching-velocity and normal acceleration responses to pulse-type elevator inputs have been analyzed to obtain frequency responses and numerical values of the coefficients of the transfer functions. These coefficients are plotted as functions of Mach number over the Mach number range of 0.59 to 1.05. All flight data were recorded at an altitude of approximately 35,000 feet, and effects of altitude variations on the frequency-response characteristics are calculated.

Also presented are the pitching-velocity frequency responses to displacements of the adjustable stabilizer. These were computed using experimentally determined values of the ratio of stabilizer effectiveness to elevator effectiveness.

A graphical method for determining transfer coefficients from frequency-response data is described. This method eliminates lengthy numerical culculations usually associated with this type of problem. An electronic analogue computer was used in conjunction with the above method so that the graphically determined results could be modified until the output of the computer matched the original flight data.

INTRODUCTION

In the design of automatic-control equipment for high performance aircraft, it is necessary to consider the dynamic-response

characteristics of the aircraft. These characteristics can be conveniently expressed as transfer functions which are expressions that describe the motion of the airplane for the various flight conditions of interest. Often these expressions can be predicted by using stability derivatives obtained from theoretical studies and from wind-tunnel tests. In many cases, however, particularly in the transonic speed range, it is necessary to resort to actual flight-test procedures in order to determine the airplane frequency response from which the desired transfer functions may be obtained.

Presented herein is one phase of a flight-test program being conducted by the NACA for the purpose of determining longitudinal, lateral, and directional frequency-response characteristics of a 35° swept-wing airplane. This report considers only the longitudinal case and presents variations of the coefficients of the transfer functions over the Mach number range of 0.59 to 1.05 for one flight altitude. The results of this phase of the test program were determined from flight data similar to that described in reference 1 and this report may be considered as an extension thereof.

A second objective is the presentation of a general method for obtaining transfer functions from frequency-response data utilizing a special set of templates and an electronic analogue computer. The templates afford a means of rapid determination of the form of the transfer functions as well as good approximations of the numerical coefficients involved. The analogue computer may then be used to modify these numerical values and to check them against the flight measurements.

NOTATION

C_L	lift coefficient
C_m	pitching-moment coefficient about airplane center of gravity
I_y	moment of inertia about the lateral axis through the center of gravity, slug-feet squared
K_1, K_2	amplitude scale factors
M	Mach number
S	wing area, square feet
T	time interval, seconds
V	flight velocity, feet per second
a	sonic velocity, feet per second

c	mean aerodynamic chord of wing, feet
g	acceleration due to gravity, feet per second squared
i_t	angle of incidence of horizontal tail, radians
m	mass, slugs
n	normal acceleration, feet per second squared (unless otherwise noted)
p	the operator $\left(\frac{d}{dt}\right)$
q	pitching velocity, radians per second
t	time, seconds
α	angle of attack, radians
δ	elevator deflection, radians (unless otherwise noted)
ρ	atmospheric density, slugs per cubic foot
$\frac{\rho V^2}{2}$	dynamic pressure, pounds per square foot
ζ	damping ratio
τ	characteristic time, seconds
ω	frequency, radians per second
ω_n	undamped natural frequency, radians per second
$\dot{\alpha}$	$\frac{d\alpha}{dt}$
$\dot{q}$	$\frac{dq}{dt}$
C_{L_α}	$\frac{dC_L}{d\alpha}$
C_{L_δ}	$\frac{dC_L}{d\delta}$

C_{m_α} $\dfrac{dC_m}{d\alpha}$

C_{m_δ} $\dfrac{dC_m}{d\delta}$

C_{m_q} $\dfrac{dC_m}{d(qc/2V)}$

$C_{m_{\dot{\alpha}}}$ $\dfrac{dC_m}{d(\dot{\alpha}c/2V)}$

M_α $\frac{1}{2}\rho V^2 Sc\, C_{m_\alpha}$

$M_{\dot{\alpha}}$ $\frac{1}{4}\rho V Sc^2\, C_{m_\alpha}$

M_q $\frac{1}{4}\rho V Sc^2\, C_{m_q}$

Z_α $-\frac{1}{2}\rho V^2 S\, C_{L_\alpha}$

Z_δ $\frac{1}{2}\rho V^2 S\, C_{L_\delta}$

TEST EQUIPMENT

The test airplane was a standard North American F86A-5 with external booms added as shown in figures 1 and 2. The physical characteristics and instrumentation of this airplane are described in reference 1. Of particular importance to the analysis used in the present report is the dynamic behavior of the instruments used to record pitching velocity and normal acceleration. Pitching velocity was measured by a rate gyro with direct optical recording. The natural frequency of this instrument was 10.0 cycles per second and the damping ratio was 0.67. Normal acceleration was measured by a standard NACA air-damped vane-type accelerometer with a natural frequency of 14.7 cycles per second and a damping ratio of 1.95.

TEST PROCEDURE AND ANALYSIS

The procedure used in the determination of the airplane frequency response and corresponding transfer functions can be divided into four distinct steps; namely, flight measurements, frequency-response computations, determination of transfer coefficients, and a final check utilizing an analogue computer. These steps are outlined in the following sections.

Flight Measurements

Transient responses of pitching velocity and normal acceleration to pulse-type elevator inputs were recorded over the Mach number range of 0.59 to 1.05. All flights were made at an altitude of 35,000 feet at values of trim lift coefficient that varied from 0.35 to 0.12. Sample time histories are shown in figure 3.

To insure consistent data, the airplane was trimmed so that variations in speed and altitude during each run were held to a minimum. To attain test speeds greater than 0.95 Mach number, it was necessary to dive the airplane, thus causing small altitude changes during these runs. In all tests, after applying the elevator pulse, the control was held fixed until the transient response was completely damped. As a check on accuracy, at least two flight records were taken at each speed.

The magnitudes of the applied elevator pulses generally varied from 10° to 12°, measured from trim position as shown in figure 4. It is desirable to use large inputs so that the transient responses can be more accurately measured. On the other hand, the analysis methods presented herein are valid only for linear systems. The input magnitudes, therefor, should be limited to a range in which the pertinent aerodynamic derivatives are essentially linear. Figure 4 shows the trim elevator angle at each flight-test condition in addition to the absolute magnitude of the input pulse. Figure 5 shows the corresponding trim angles of attack and the maximum and minimum angles reached during the oscillations that followed each elevator pulse.

A transient-type input, in particular a pulse, was used in these tests mainly because it enables an entire airplane frequency response to be computed from one flight run of a few seconds duration. Sinusoidal elevator inputs could have been used to determine the steady-state frequency response (amplitudes and phase angles) directly and thus eliminate the calculations described in the following paragraphs. The use of this type of input was not considered to be feasible because of the large amount of flight time required inasmuch as only one point on the

frequency-response curve could be obtained from each flight run. In addition it would require the installation of special sine-wave generating equipment in the airplane.

Frequency-Response Computations

The next step in the analysis is the conversion of the transient time histories into the frequency domain.

Under certain conditions a time function such as the pitching velocity $q(t)$ can be transformed into a complex frequency function $q(i\omega)$ by means of the Fourier integral relation

$$q(i\omega) = \int_0^\infty q(t)\, e^{-i\omega t}\, dt \tag{1}$$

This integral must be evaluated from time zero to infinity for each frequency ω at which $q(i\omega)$ is desired. Obviously, the integration can be accomplished only if the behavior of $q(t)$ is known for an infinite time. Since $q(t)$ can be measured only for a finite time T, it is necessary for the system to reach steady-state conditions before time T such that $q(t)$ may be expressed analytically between the time limits T and infinity. In addition, the product $q(t)e^{-i\omega t}$ must converge as t approaches infinity.

Examination of the data used in this analysis showed that in every case the forcing function $\delta(t)$ and the responses $q(t)$ and $n(t)$ became constant after a finite time interval T. These steady-state values may be expressed as δ_T, q_T, and n_T, respectively, and thus equation (1) may be divided into two parts as follows:

$$q(i\omega) = \int_0^T q(t)\, e^{-i\omega t}\, dt + q_T \int_T^\infty e^{-i\omega t}\, dt$$

The second integral can be evaluated analytically so that

$$q(i\omega) = \frac{q_T}{i\omega}\, e^{-i\omega T} + \int_0^T q(t) e^{-i\omega t}\, dt \tag{2}$$

For computational purposes equation (2) may be divided into its real and imaginary parts represented by the symbols R.P. and I.P., respectively, so that

$$q(i\omega) = (\text{R.P.}) + i(\text{I.P.})$$

where

$$\text{R.P.} = -\frac{q_T}{\omega}\sin \omega T + \int_0^T q(t)\cos \omega t\, dt$$

$$\text{I.P.} = -\frac{q_T}{\omega}\cos \omega T - \int_0^T q(t)\sin \omega t\, dt$$

The two integrals involving the transient part of $q(t)$ may be evaluated by any of several approximation methods. In analyzing the data of this report, Simpson's rule was used to find the area under the product curves $q(t)\cos \omega t$ and $q(t)\sin \omega t$. Values of $q(t)$ were tabulated at 0.05-second intervals and the integrations were carried out at each integral value of frequency from 1 to 10 radians per second.

After obtaining the numerical values of R.P. and I.P. at each frequency, $q(i\omega)$ can be expressed in polar notation such that

$$q(i\omega) = |q|\, e^{i\varphi_q}$$

where the amplitude, $|q| = \sqrt{(\text{R.P.})^2 + (\text{I.P.})^2}$ and the angle, $\varphi_q = \arctan \text{I.P.}/\text{R.P.}$

The above integration process was repeated for the elevator forcing function $\delta(t)$ to determine

$$\delta(i\omega) = |\delta| e^{i\varphi_\delta}$$

Then the ratio of q/δ was determined as

$$\frac{q}{\delta}(i\omega) = \frac{q(i\omega)}{\delta(i\omega)} = \left|\frac{q}{\delta}\right| e^{i(\varphi_q - \varphi_\delta)} = \left|\frac{q}{\delta}\right| e^{i\varphi_{q/\delta}}$$

where $|q/\delta|$ is the amplitude ratio and $\varphi_{q/\delta}$ is the phase difference between the two quantities, $\varphi_q - \varphi_\delta$.

Similar calculations were made using the normal acceleration time histories in order to obtain the quantities $|n/\delta|$ and $\varphi_{n/\delta}$.

The final result of the above calculations is a graphical representation of the airplane transfer function (frequency response) for a given test condition. This is plotted as curves of amplitude ratio and phase angle versus frequency. The remainder of this section of the report is concerned with the determination of analytical expressions for these curves.

Reference 2 is one of many sources that explain in more detail the use of the Fourier transform for problems of this type.

Determination of Transfer Coefficients

A graphical method was used to find the type of transfer functions that best define the measured q/δ and n/δ frequency responses. Numerical values of the transfer coefficients were also determined in the same operation. This method involved the use of a set of templates developed by C. S. Draper of the Instrumentation Laboratory of the Massachusetts Institute of Technology. These templates are described fully in reference 3. The design of the templates was based on the following considerations:

1. A rational function of complex frequency p can, in general, be expressed as

$$F(p) = K \frac{(p+a_1)(p+a_2) \cdot \cdot \cdot (p+a_n)}{(p+b_1)(p+b_2) \cdot \cdot \cdot (p+b_m)} \tag{3}$$

where the a_i and b_i may be either real or complex, and, if complex, always appear as conjugate pairs and where K is any real number. When a_i is a real number, a factor $(p+a_i)$ may be expressed as

$$\frac{1}{\tau}(1+\tau p)$$

where $\tau = \frac{1}{a_i}$. When a_i and a_{i+1} are a complex conjugate pair the two factors $(p+a_i)(p+a_{i+1})$ can be expanded, by introducing new coefficients, into the form $(p^2+2\zeta\omega_n p+\omega_n^2)$ where $\omega_n^2 = a_i a_{i+1}$ and $2\zeta\omega_n = a_i + a_{i+1}$. Factoring out ω_n^2 then gives

$$\omega_n^2 \left(1 + 2\zeta \frac{p}{\omega_n} + \frac{p^2}{\omega_n^2}\right)$$

The terms $\frac{1}{\tau}$ and ω_n^2 that appear outside the parentheses, being real numbers, may be grouped together with the multiplying factor K. When an a_i or b_i is zero then a factor p will be present in either the numerator or the denominator. Then, $F(p)$ in factored form will consist entirely of combinations of the three forms.

Since we are interested only in the steady-state frequency response, the complex variable p can be replaced by the frequency variable $i\omega$, and each of the three factors may be written in polar form as follows:

For $(1+\tau p)$,

$$1 + \tau i\omega = \sqrt{1+\tau^2\omega^2}\, e^{i\varphi_1} \tag{4}$$

where

$$\varphi_1 = \tan^{-1} \tau\omega$$

for $\left(1 + 2\zeta \frac{p}{\omega_n} + \frac{p^2}{\omega_n{}^2}\right)$,

$$1 + 2\zeta \frac{i\omega}{\omega_n} + \left(\frac{i\omega}{\omega_n}\right)^2 = \sqrt{\left(1 - \frac{\omega^2}{\omega_n{}^2}\right)^2 + 4\zeta^2 \frac{\omega^2}{\omega_n{}^2}}\, e^{i\varphi_2} \tag{5}$$

where

$$\varphi_2 = \tan^{-1} \frac{2\zeta\left(\omega/\omega_n\right)}{1 - \left(\omega^2/\omega_n{}^2\right)}$$

and for p

$$i\omega = \omega e^{i\varphi_3} \tag{6}$$

where

$$\varphi_3 = \tan^{-1}\infty = 90^\circ$$

2. When $\tau\omega$ is taken as a nondimensional frequency variable all first-order terms of the form $(1 + \tau i\omega)$ can be defined by a single amplitude curve and a single phase-angle curve as shown in figure 6. In a similar manner all possible second-order terms of the form $1 + 2\zeta\frac{i\omega}{\omega_n} + \left(\frac{i\omega}{\omega_n}\right)^2$ can be defined by a family of curves with ω/ω_n as the nondimensional frequency variable. There will be a different pair of curves for each value of damping ratio ζ, as shown in figure 7. The factor $i\omega$ has not been plotted because (from equation (6)) its amplitude is simply equal to ω and the phase angle is a constant 90°.

3. Since a typical transfer function may consist of more than one of these factors in both numerator and denominator, it is of great advantage to plot the amplitudes to a logarithmic scale so that multiplication or division of factors of the type shown in equations (4) to (6) may be accomplished by mere graphical addition of the amplitudes. The nondimensional frequency has also been plotted to a logarithmic scale as shown in figures 6 and 7. Then as frequency approaches either zero or

infinity the amplitudes become asymptotic to straight lines. In both figures as frequency decreases the amplitudes approach asymptotically the value of unity. At high frequencies the amplitude of $(1 + \tau i\omega)$ is essentially equal to $\tau\omega$ and thus it plots as a straight line of slope 1 (fig. 6). Similarly, the amplitude of a second-order term approaches the value $(\omega/\omega_n)^2$ as frequency increases and is asymptotic to a straight line of slope 2. Since a second-order term of this type normally appears in the denominator, it has been plotted as

$$\left[1 + 2\zeta\frac{i\omega}{\omega_n} + \left(\frac{i\omega}{\omega_n}\right)^2\right]^{-1}$$

and thus the slope of the amplitude curve is -2 (fig. 7). In both plots the asymptotes intersect at unity on the nondimensional frequency scale. This intersection is termed "the breakpoint."

The phase angles are plotted to a linear scale because when factors of the types shown in equations (4) to (6) are combined, the resultant phase angle of $F(p)$ is merely the algebraic sum of the individual angles. It can be seen in figures 6 and 7 that the angles of these first- and second-order terms approach 90° and -180°, respectively, at high frequencies. Thus an amplitude slope of 1 corresponds to an angle of 90°, while a slope of -2 corresponds to an angle of -180°. In general, as ω approaches infinity the amplitude of $F(p)$ approaches $K\omega^{(n-m)}$, where n and m are defined in equation (3). Then the amplitude slope is equal to $(n-m)$ on the logarithmic plot and the phase angle is $90(n-m)^\circ$.

The templates used in the analysis of the data were accurate representations of the curves shown in figures 6 and 7 cut from transparent material with the breakpoints marked. Twelve pairs of second-order templates were included in the set to give values of damping ratio from 0.1 to 1.0 in increments of 0.1 and in addition values of 0.05 and 0.15.

The computed frequency-response data (amplitude ratios and phase angles) were plotted to the same logarithmic scale as the templates, and then by a trial-and-error approach the template or combination of templates that best matched the given data was determined. To determine the proper combination, various amplitude templates were positioned in such a way that their algebraic sum matched the experimental amplitude ratio curve. For each amplitude template the corresponding phase-angle template was placed on the experimental phase-angle curve so that the breakpoint of each pair was alined with respect to frequency. The various pairs of templates were then adjusted until the sum of the individual amplitudes and phase angles most nearly matched the test data. The frequency at which the breakpoint of each pair occurred (ω_{Bp}) was

noted and then the appropriate values of τ and ω_n were determined directly, since for each first order term

$$\tau = \frac{1}{\omega_{Bp}}$$

and for each second-order term

$$\omega_n = \omega_{Bp}$$

In general, each factor will have a different breakpoint.

At first glance, this procedure may seem extremely tedious but it has been found that with practice one can determine coefficients quite rapidly in this manner. For a more complete description of the principles involved in this type of graphical representation reference 4 is recommended.

Final Check

As a final step in the calculations a Reeves analogue computer was used to check the results of all previous computations. This was accomplished by placing the actual time histories of elevator-control motion into the computer by means of an input table. Then this input was fed into a circuit representing the equations of motion as obtained in the previous step and the outputs of the machine were obtained. These outputs were compared to the actual time histories of pitching velocity and normal acceleration obtained in flight. By changing dial settings on the computer the transfer coefficients could be adjusted until the output of the computer most nearly matched the actual flight data. (Such a comparison is shown in fig. 3.) Thus, in addition to checking the calculations, this step actually resulted in a refinement of the coefficients obtained with the templates. In general, operations of this type can be conveniently accomplished on the computer only when the form of the transfer function is known.

RESULTS AND DISCUSSION

The results presented in the following paragraphs were obtained from transient time histories such as shown in figure 3 by the methods described in the previous section. Discussed here are the airplane frequency-response curves and the actual transfer functions that define these curves. Also presented as supplementary results are the Mach

number variations of elevator effectiveness and the effect of altitude on the transfer coefficients.

Frequency–Response Curves

Plotted in figures 8 and 9 are frequency–response amplitude and phase–angle curves of both pitching–velocity and normal–acceleration responses to elevator inputs for several different Mach numbers. Although two records were analyzed at each flight speed, the results of only one have been plotted. The agreement between the two results at each Mach number was generally good with variations in amplitude ratio rarely exceeding 5 percent of their maximum values, while the differences in phase angle were usually less than 5°.

The pitching–velocity frequency–reponse amplitudes of figure 8(a) show an increase in natural frequency with Mach number and also a reduction in amplitude ratios above a Mach number of 0.76, indicating a decrease in elevator effectiveness. The normal–acceleration frequency–response amplitudes of figure 9(a) show, in general, the same characteristics with some irregularities at the higher flight speeds. Figures 8(b) and 9(b) show the corresponding phase–angle variations with Mach number.

Each transient reponse was analyzed at integral values of frequency from 1 to 10 radians per second. In some cases, however, there appeared to be inconsistencies in the calculated responses at either end of the frequency range where the magnitude of the response was small. This was particularly evident over the low–frequency parts of the normal–acceleration responses obtained at the higher flight speeds. For this reason, as well as for clarity, portions of some of the responses have been omitted from figures 8 and 9. In general, the pitching–velocity data are considered more reliable than the acceleration data because the dynamic characteristics possessed by the rate gyro were superior to those of the accelerometer.

In figure 10 is plotted a series of amplitude–ratio curves of pitching–velocity responses to inputs of an adjustable stabilizer control for various Mach numbers. These plots were obtained by multiplying the amplitude curves of figure 8(a) by values of $d\delta/di_t$ obtained from static flight tests and shown in figure 11. Figure 10 illustrates the type of responses that would have been obtained if the stabilizer had been used as the maneuvering control and there is no indication of the large decrease in control effectiveness previously noted in figure 8(a). For these calculations the phase angles for the q/i_t response are the same as those shown in figure 8(b).

Transfer Functions

The airplane transfer functions were determined from q/δ and n/δ frequency responses (figs. 8 and 9) by using the templates described in the Analysis section. Final values of the coefficients were obtained from the analogue computer by matching the original time histories. The transfer functions for this particular airplane were found to be of the following form:

$$\frac{q}{\delta}(i\omega) = K_1 \frac{1 + \tau i\omega}{1 + 2\zeta\left(i\omega/\omega_n\right) + \left(i\omega/\omega_n\right)^2}$$

$$\frac{n}{\delta}(i\omega) = K_2 \frac{1}{1 + 2\zeta\left(i\omega/\omega_n\right) + \left(i\omega/\omega_n\right)^2}$$

As indicated by figure 3, these equations adequately define the transient motion of the airplane as measured in flight. These equations are also of the same form as the theoretical transfer functions developed in appendix A.

The Mach number variations of the coefficients ω_n, ζ, τ, K_1 and K_2 are plotted in figures 12 and 13. The damping ratio curve of figure 12 was faired by referring to the damping coefficient curve plotted in reference 1 where more data were available to define the sharp variations between Mach numbers of 0.88 to 0.95. An indication of the consistency of the measurements and calculations is given by the scatter of the points at each flight speed. The coefficients ζ and ω_n were determined directly from the q/δ response and then were verified using the n/δ response.

In determining the transfer coefficients of the q/δ response there was some uncertainty as to the best values for τ and K_1. It was found that in some cases the test data could be equally well satisfied by a range of values of these two coefficients. For example, a decrease in τ could be compensated for by an increase in K_1 such that the product $K_1\tau$ remained constant. Examination of the q/δ transfer function will indicate the reason for this indeterminacy. When expressed in polar form the numerator of the amplitude ratio $|q/\delta|$ is

$$K_1\sqrt{1 + \tau^2\omega^2}$$

It can be seen that as frequency increases $\tau^2\omega^2$ becomes large compared to unity, and the numerator may be approximated simply by $K_1\tau\omega$. Thus it appears that $K_1\tau$ is the most essential quantity in the numerator of

the q/δ transfer function and this has been plotted in figure 14. The results in this form exhibit less scatter than the individual coefficients K_1 and τ shown in figure 13.

Elevator Effectiveness

Also plotted in figure 14 is the variation with Mach number of the elevator effectiveness C_{m_δ} computed directly from the product $K_1\tau$ as described in appendix B. This quantity is compared to wind-tunnel values obtained from reference 5, and also to unpublished static flight data. The agreement between the three curves is generally good. There is some scatter, however, in the test points computed herein which may be attributed to the nonlinearities that are discussed in the section on accuracy. The method used here is not suggested as a means for determining C_{m_δ} since this can usually be obtained more directly from static flight measurements. However, the computation is justified as an additional check on the validity of the methods used in this report.

Altitude Variations

Since the data presented in this report were all obtained at an altitude of approximately 35,000 feet, calculations, as described in appendix C, were made to show the effects of changes in altitude on the frequency-response characteristics of the airplane. The results of these calculations are plotted in figure 15, which shows the variation at constant Mach number and at constant lift coefficient of each of the transfer coefficients over an altitude range of from sea level to 50,000 feet. Calculations based on these curves would be valid only at Mach numbers where altitude variations do not result in departures from the linear range of the lift curve.

In figure 16 are plotted typical pitching-velocity frequency-response curves calculated for the test airplane at a Mach number of 0.81 for altitudes of sea level, 15,000 and 35,000 feet. It can be seen that as altitude increases both the amplitude and natural frequency are reduced. Calculations for normal-acceleration response would show similar tendencies with possibly even greater changes in amplitude.

ACCURACY

In order to assess the accuracy of experimentally determined transfer coefficients, consideration must be given to certain basic factors

that affect the solution of this type of problem. The templates will indicate the type of transfer function that best fits a set of experimental data over a particular frequency range. Changing the width of the frequency spectrum analyzed will, in many cases, not only change the values of the coefficients but also change the type of the transfer function. This would be true in general of a system that has more than one well-defined mode of motion. The airplane falls into this category.

In the analysis of this report only a narrow frequency band was considered. This band bracketed the resonant peak of the short-period mode and thus, as would be expected by theory, the templates showed the system to have essentially two degrees of freedom (a second-order transfer function). If flight data had been obtained that would be suitable for analysis at lower frequencies, then we would have expected the system to be more closely represented by a fourth-order transfer function that would have included the long-period (phugoid) mode in addition to the short-period mode mentioned above. Similarly, if the analysis had included very high frequencies, one or more vibration or flutter modes might have further complicated the resultant transfer function.

Other factors that affect the accuracy and consistency of the computed transfer coefficients are discussed in the following paragraphs.

Nonlinearities

The analysis used in this report is based on the assumption of linear behavior of all aerodynamic derivatives, thus implying that the frequency response and the related transfer coefficients are completely independent of the shape and magnitude of the forcing function. In calculating the dynamic-response characteristics of aircraft, this assumption is generally valid, provided that only small disturbances from trimmed flight are considered. There may be cases, however, where nonlinear derivatives exist even under these conditions. Then, at each flight speed and altitude, the computed frequency responses will vary in some manner with the type of control input used and also with the magnitude of the input. This will lead to corresponding variations in the calculated transfer coefficients, and in extreme cases it may be impossible to find a set of linear coefficients that adequately describe the transient flight data.

Investigation has shown that, in the test airplane, the variation of pitching moment with elevator angle tends to become nonlinear (C_{m_δ} decreases) as the angle is increased above a certain value. Unpublished data have demonstrated this fact at a Mach number of 0.80 where airplane responses to pulses of varying magnitude were recorded. It was found also that the amplitude ratio of the frequency response

decreased slightly as the magnitude of the pulse was increased. The only coefficients appreciably affected were K_1 and K_2. The variations in K_1 resulted in similar variations in the calculated values of C_{m_δ} which are in effect linear approximations of the true nonlinear curves.

The results of this report indicate the same nonlinear effects. At several different speeds (such as 0.69 Mach number) variations in the coefficients K_1 and K_2, shown in figure 13, were directly traceable to variations in the sizes of the input pulses (fig. 4). For the most part these effects were small.

From the equations developed in appendix A it can be seen that, through the frequency range of interest, both $|q/\delta|$ and $|n/\delta|$ are approximately proportional to C_{m_δ}. Thus it is reasonable to expect only the multiplying factors K_1 and K_2 to be affected by the simple nonlinearity in C_{m_δ}.

There was no evidence of nonlinearities in any of the other stability derivatives.

Instrumentation

The dynamic characteristics of the recording instruments are of great importance. Each instrument has its own frequency response which must be considered in determining the true airplane response. Furthermore, the natural frequency of the instrument definitely limits the highest frequency at which the data may be analyzed.

Any tendency on the part of a recording instrument to drift with time would result in erroneous steady-state values of the airplane response (errors in the low-frequency region).

The rate gyro used in this test program was found to have satisfactory dynamic amplitude characteristics, and corrections were applied only to account for instrument lag. The linear accelerometer had less desirable dynamic characteristics because of its extremely high damping ratio (1.95) which normally means that amplitude as well as phase-angle corrections must be made; but, because the normal acceleration data are of only secondary importance to this report, the performance of the instrument was considered to be adequate even though amplitude corrections were not made. There was no evidence of drift with time in either instrument.

Flight Technique

As mentioned previously, it was necessary to dive the airplane in order to obtain records at the highest speeds, which resulted in changes in both speed and altitude. These changes increase the difficulty in finding a set of coefficients that will describe the response of the airplane. Inadvertent disturbances such as those caused by rough air will cause airplane motions that are not consistent with the control input and thus may result in serious discrepancies in the airplane frequency response.

Data Reduction

The most likely source of error in the data reduction is the film-reading operation. However, such random errors should only affect the high-frequency part of the response, provided that the steady-state portion of the transient records is carefully measured.

The use of Simpson's Rule in obtaining the Fourier integrals of the transient records was found to be a highly accurate method, provided that the time history is evaluated at small enough time intervals. Unpublished work has shown that if a time interval of 0.05 second is used, then transient records of the type shown in this report can be analyzed to frequencies as high as 12 radians per second with errors of less than 1 percent. In general, the time interval should be small enough so that each cycle of the product curves $q(t) \sin \omega t$ and $q(t) \cos \omega t$ can be defined by at least six measurements.

In using the templates to determine transfer coefficients it was generally not possible to exactly match the damping ratio of an experimental frequency-response curve with any of the available second-order templates. This type of error could be minimized by expanding the set to include more intermediate values of ζ. In any event the damping ratio can be corrected by making use of the analogue computer as mentioned previously.

CONCLUDING REMARKS

The primary objective of this report is the presentation of dynamic longitudinal-stability characteristics of a 35° swept-wing airplane as determined from transient flight data. A secondary objective is the presentation of a method that enables these characteristics to be expressed in the form of airplane transfer functions for each flight

condition. Time histories of pitching-velocity and normal-acceleration responses to pulse-type elevator inputs were satisfactorily analyzed by means of the Fourier integral transformation to obtain the airplane frequency responses in graphical form. The equations or transfer functions that most nearly matched these curves were then readily determined by means of special templates. The analogue computor was useful in obtaining more satisfactory numerical coefficients of the transfer functions and in checking all intermediate calculations against the original flight measurements.

Examination of the pitching-velocity frequency-response curves for elevator-control inputs shows decreasing amplitude ratios as Mach number is increased above 0.76, indicating low elevator effectiveness in the transonic range. This large reduction in amplitude is not evident, however, when the stabilizer is used as the manuevering control.

Each of the computed transfer coefficients shows some irregularity at or near the Mach number of 0.92. Otherwise the following trends are evident:

The undamped natural frequency ω_n increases with Mach number. The damping ratio ζ at 35,000 feet decreases from 0.38 at a Mach number of 0.8 to 0.15 at a Mach number of 1.0. The coefficients τ, K_1, and K_2 each show, in general, a decrease with increasing Mach number through the transonic speed range. The elevator effectiveness parameter C_{m_δ} computed from experimental values of τ and K_1 decreases rapidly from 0.35 to 0.06 between Mach numbers of 0.8 and 1.0.

It is shown that the effect of altitude changes on the transfer coefficients is such as to cause a decrease in the amplitude and natural frequency of the airplane response with increasing altitude.

Ames Aeronautical Laboratory,
National Advisory Committee for Aeronautics,
Moffett Field, California.

APPENDIX A

RELATIONSHIP BETWEEN EXPERIMENTALLY DETERMINED TRANSFER FUNCTIONS AND THEORETICAL EQUATIONS OF MOTION

If the longitudinal equations of motion of the airplane in level flight at constant speed are assumed to be of the following form:

$$mV(\dot{\alpha} - q) = Z_\alpha \alpha + Z_\delta \delta$$

and

$$I_y \dot{q} = M_q q + M_\alpha \alpha + M_{\dot{\alpha}} \dot{\alpha} + M_\delta \delta$$

they can be solved simultaneously to give

$$\frac{q}{\delta} = \frac{C_{o_q} + C_{1_q} p}{p^2 + bp + k} \tag{A1}$$

where p is the operator $\frac{d}{dt}$, and where

$$k = \frac{Z_\alpha M_q}{mVI_y} - \frac{M_\alpha}{I_y} \tag{A2}$$

$$b = -\frac{Z_\alpha}{mV} - \frac{M_q + M_{\dot{\alpha}}}{I_y} \tag{A3}$$

$$C_{o_q} = \frac{Z_\delta M_\alpha - M_\delta Z_\alpha}{mVI_y} \tag{A4}$$

$$C_{1_q} = \frac{Z_\delta M_{\dot{\alpha}}}{mVI_y} + \frac{M_\delta}{I_y} \tag{A5}$$

It was shown in this report that the experimentally determined pitching-velocity responses may be represented by equations of the form

$$\frac{q}{\delta} = K_1 \frac{1 + \tau p}{1 + 2\zeta\left(p/\omega_n\right) + \left(p^2/\omega_n{}^2\right)}$$

By rearranging terms this equation may be expressed as

$$\frac{q}{\delta} = \frac{K_1 \omega_n^2 + K_1 \omega_n^2 \tau p}{p^2 + 2\zeta \omega_n p + \omega_n^2}$$

which is of the same form as equation (A1) so that

$$k \equiv \omega_n^2 \tag{A6}$$

$$b \equiv 2\zeta\omega_n \tag{A7}$$

$$C_{o_q} \equiv K_1\omega_n^2 \tag{A8}$$

$$C_{1_q} \equiv K_1\omega_n^2\tau \tag{A9}$$

To obtain the normal-acceleration response n/δ, the two equations of motion may be solved simultaneously for α/δ. Then n/δ is obtained directly from the relation

$$\frac{n}{\delta} = V\left(\frac{\dot{\alpha}}{\delta} - \frac{q}{\delta}\right)$$

and may be expressed as

$$\frac{n}{\delta} = \frac{C_{o_n} + C_{1_n}p + C_{2_n}p^2}{p^2 + bp + k}$$

where

$$C_{o_n} = \frac{Z_\alpha M_\delta - Z_\delta M_\alpha}{mI_y}$$

$$C_{1_n} = -\frac{Z_\delta}{mI_y}(M_q + M_{\dot{\alpha}})$$

$$C_{2_n} = \frac{Z_\delta}{m}$$

Investigation has shown that for conventional aircraft the term C_{1_n} is negligible and that in most cases C_{2_n} has only a small effect on the airplane response over the low frequency range of interest. Therefore, n/δ may be expressed simply as

$$\frac{n}{\delta} = \frac{C_{o_n}}{p^2 + bp + k}$$

This equation is of the same form as the experimentally determined transfer function

$$\frac{n}{\delta} = \frac{K_2}{1 + 2\zeta\left(p/\omega_n\right) + \left(p^2/\omega_n{}^2\right)}$$

and thus C_{o_n} is identical to $K_2\omega_n{}^2$.

APPENDIX B

CALCULATION OF C_{m_δ}

The elevator effectiveness parameter C_{m_δ} can be computed directly from the experimental results of this report by making use of equations developed in appendix A. In equation (A5), the term $Z_\delta M_{\dot{\alpha}}/mVI_y$ is, for conventional aircraft, very small as compared to M_δ/I_y, and thus M_δ may be approximated simply as $I_y C_{l_q}$. Then from equation (A9) M_δ can be expressed as

$$M_\delta = I_y K_1 \omega_n^2 \tau$$

Finally from the definition of M_δ,

$$C_{m_\delta} = \frac{2I_y K_1 \omega_n^2 \tau}{\rho V^2 Sc}$$

APPENDIX C

ESTIMATION OF ALTITUDE EFFECTS

From the definitions of the coefficients obtained from the theoretical equations of motion, it is possible to estimate the effects of changes in altitude on the airplane frequency response. If the Mach number remains constant as altitude and density change, then the flight velocity will vary directly with the speed of sound ($V = Ma$). By neglecting some small terms and by assuming that no changes occur in the nondimensional derivatives, these coefficients may be expressed in terms of ρ and a as follows:

$$k = -\frac{M_\alpha}{I_y} = -C_{m_\alpha}\frac{\rho V^2 Sc}{2I_y} \sim \rho a^2$$

(omitting $\frac{Z_\alpha M_q}{mVI_y}$)

$$b = -\frac{Z_\alpha}{mV} - \frac{M_q + M_{\dot{\alpha}}}{I_y} = -\frac{\rho VS}{2}\left[\frac{C_{L_\alpha}}{m} + (C_{m_q} + C_{m_{\dot{\alpha}}})\frac{c^2}{2I_y}\right] \sim \rho a$$

$$C_{o_q} = \frac{Z_\delta M_\alpha - Z_\alpha M_\delta}{mVI_y} = \frac{\rho^2 V^3 S^2 c}{4mI_y}(C_{L_\delta}C_{m_\alpha} - C_{L_\alpha}C_{m_\delta}) \sim \rho^2 a^3$$

$$C_{1_q} = \frac{M_\delta}{I_y} = C_{m_\delta}\frac{\rho V^2 Sc}{2I_y} \sim \rho a^2$$

(omitting $\frac{Z_\delta M_{\dot{\alpha}}}{mVI_y}$)

$$C_{o_n} = -VC_{o_q} \sim \rho^2 a^4$$

From the identities that define the relations between the various coefficients, it can be seen that

$$\omega_n \sim a\sqrt{\rho}$$

$$\zeta \sim \sqrt{\rho}$$

$$\tau \sim \frac{1}{\rho a}$$

$K_1 \sim \rho a$

$K_2 \sim \rho a^2$

REFERENCES

1. Triplett, William C., and Van Dyke, Rudolph D., Jr.: Preliminary Flight Investigation of the Dynamic Longitudinal-Stability Characteristics of a 35° Swept-Wing Airplane. NACA RM A50J09a, 1950.

2. Gardner, Murray F., and Barnes, John L.: Transients in Linear Systems Studied by the Laplace Transformation, vol. 1. John Wiley & Sons, Inc., N.Y., 1942.

3. Lees, Sidney: Graphical Aids for the Graphical Representation of Functions of the Imaginary Argument. M.I.T., Instrumentation Lab., Engineering Memo. E-25, Feb. 1951.

4. Brown, Gordon S., and Campbell, Donald P.: Principles of Servomechanisms. John Wiley & Sons, Inc., N.Y., 1948.

5. Morrill, Charles P., Jr., and Boddy, Lee E.: High-Speed Stability and Control Characteristics of a Fighter Airplane Model with a Swept-Back Wing and Tail. NACA RM A7K28, 1948.

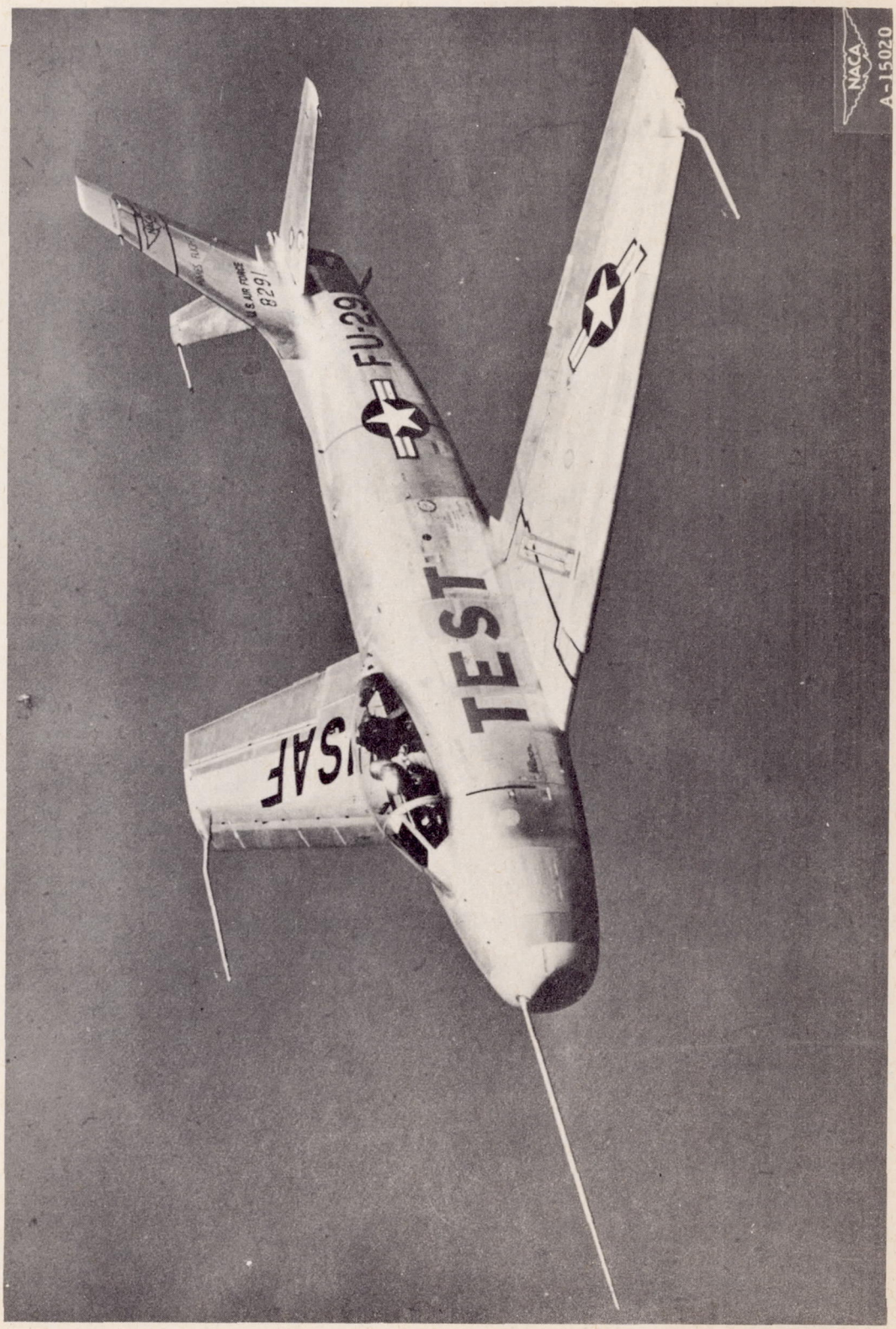

Figure 1.- Photograph of the test airplane.

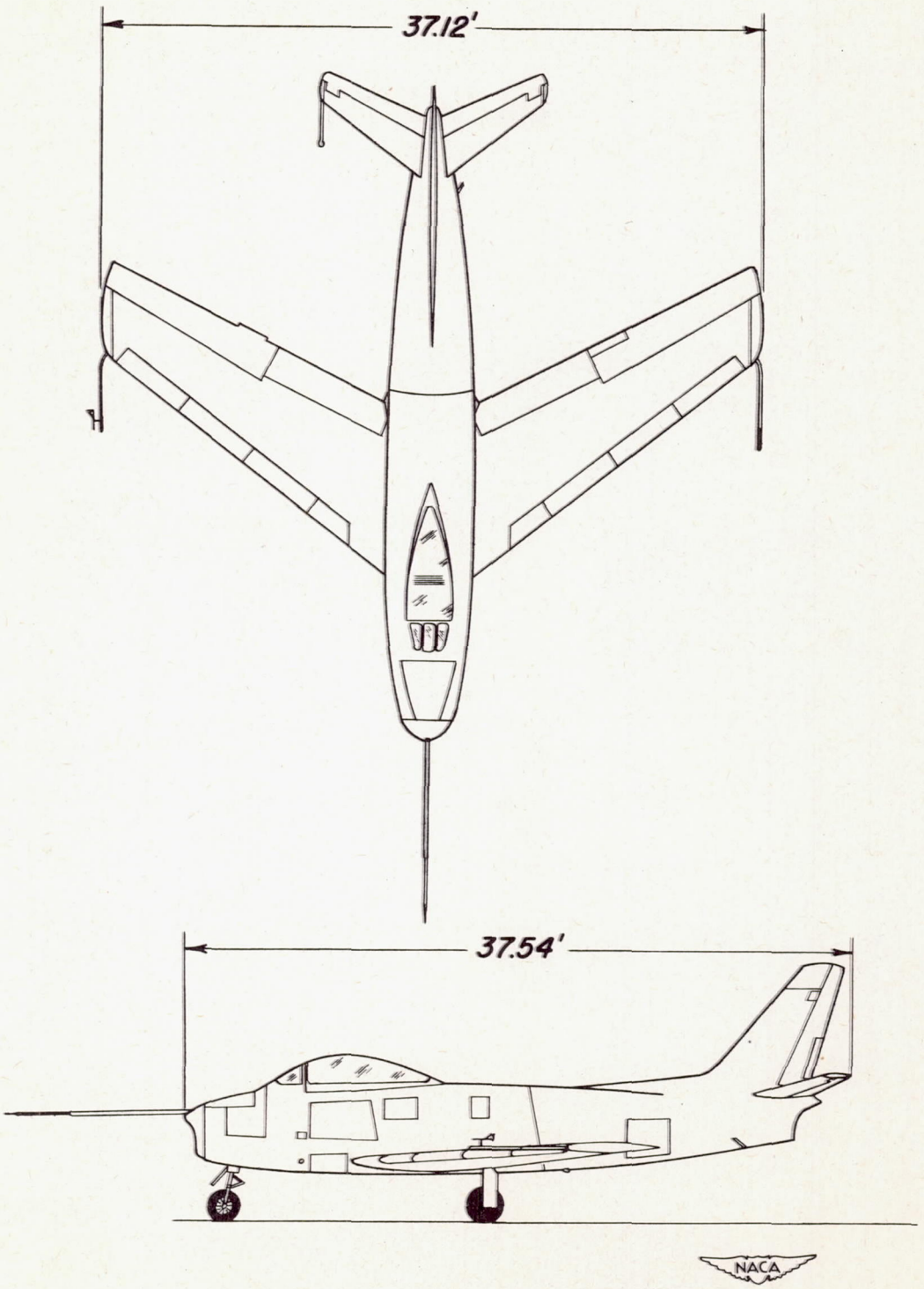

Figure 2.- Two-view drawing of the test airplane.

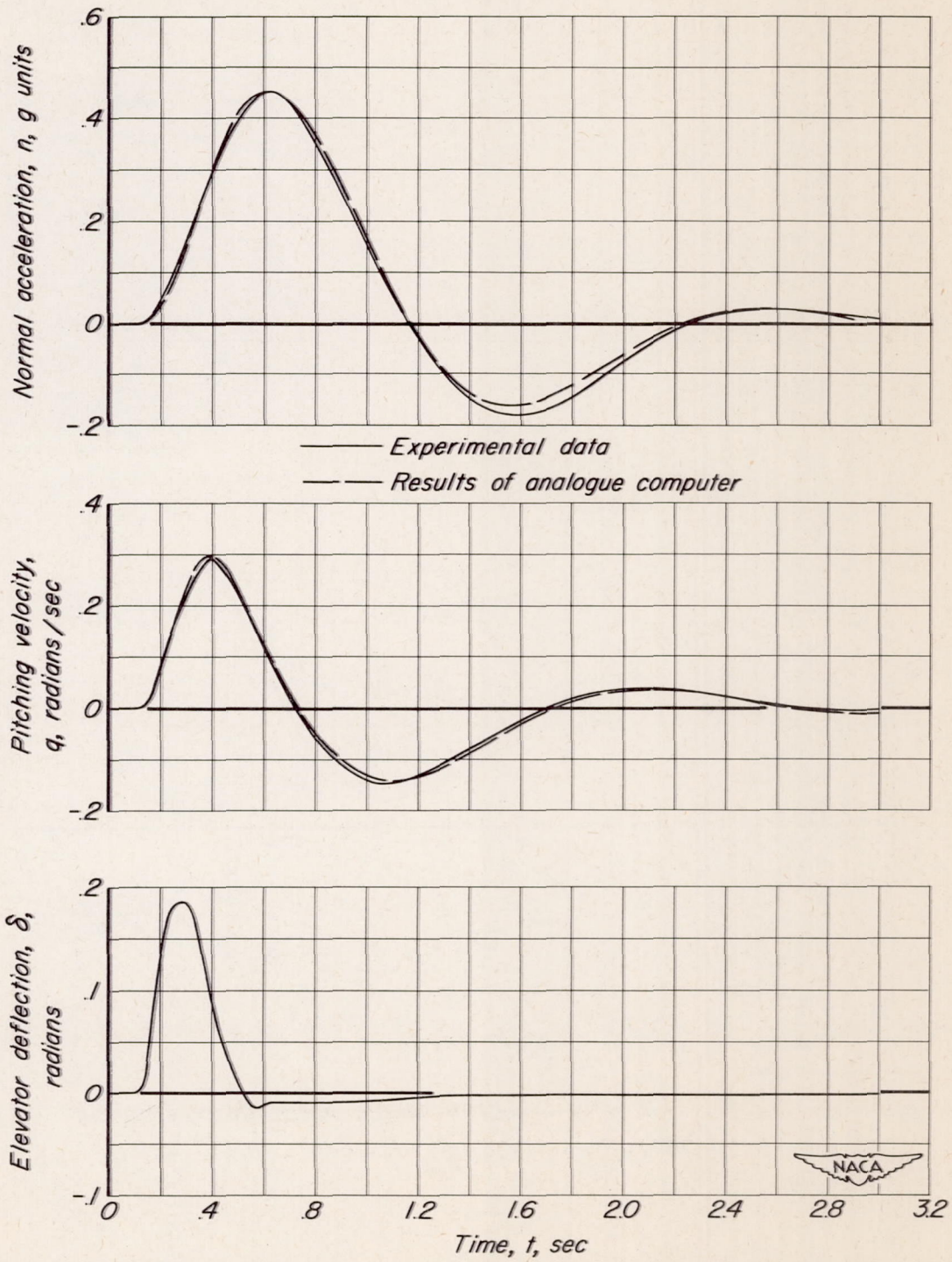

Figure 3.– Sample flight records of normal acceleration, pitching velocity, and elevator angle at Mach number of 0.81.

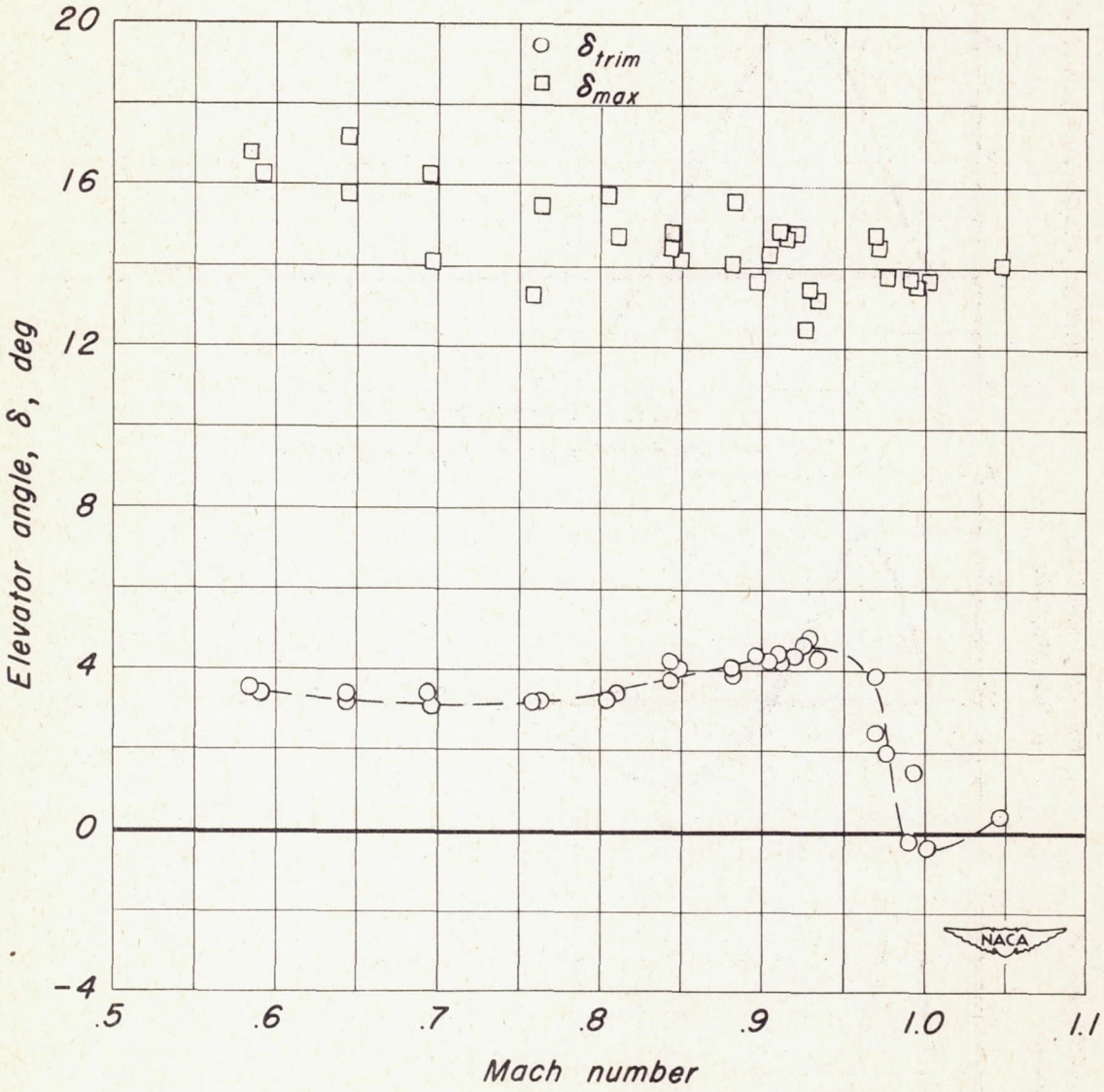

Figure 4.- Variation of trim elevator angle with Mach number and maximum elevator deflection attained during each maneuver.

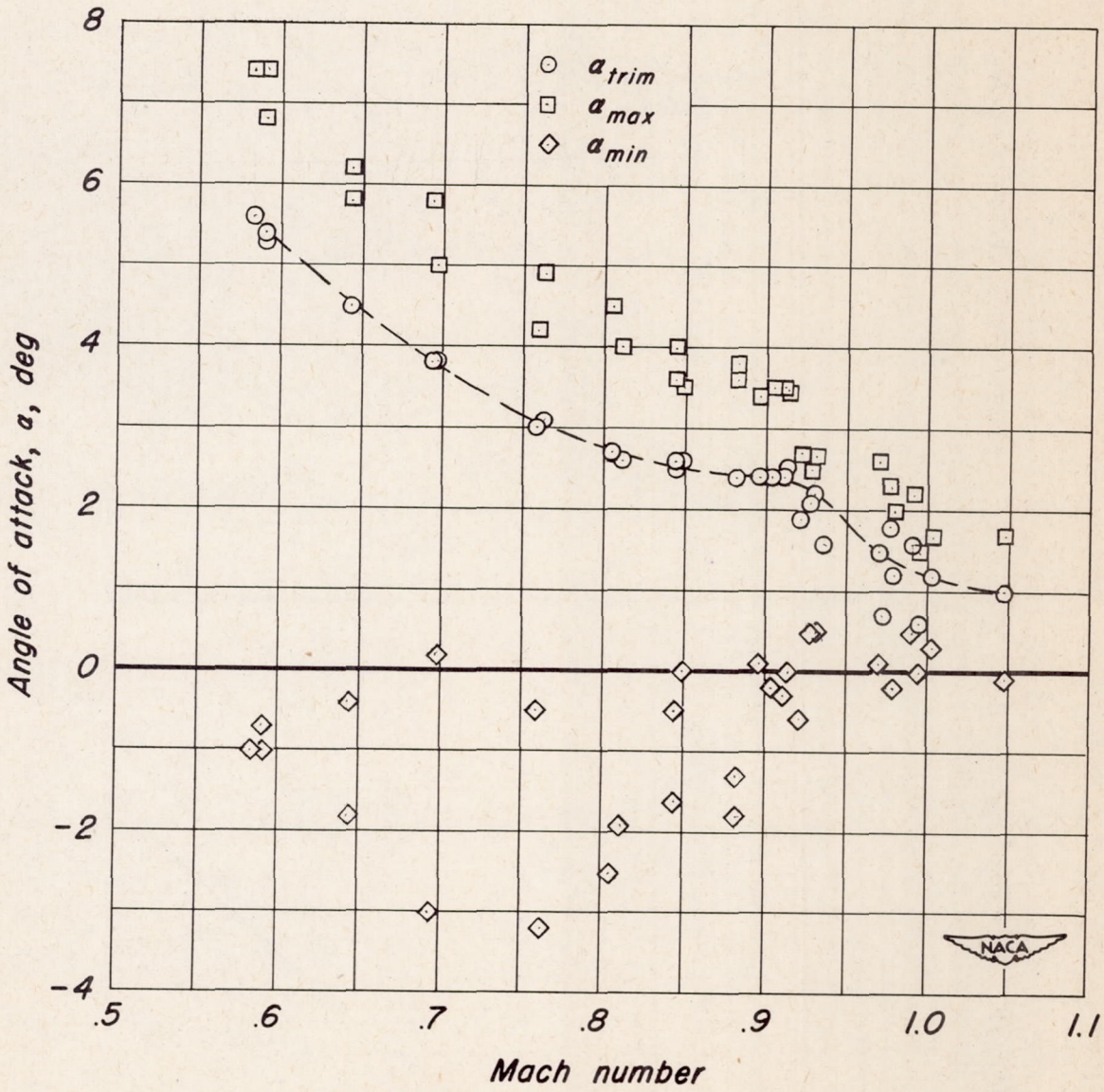

Figure 5.- Variation of trim angle of attack with Mach number and the maximum and minimum angles following each elevator pulse.

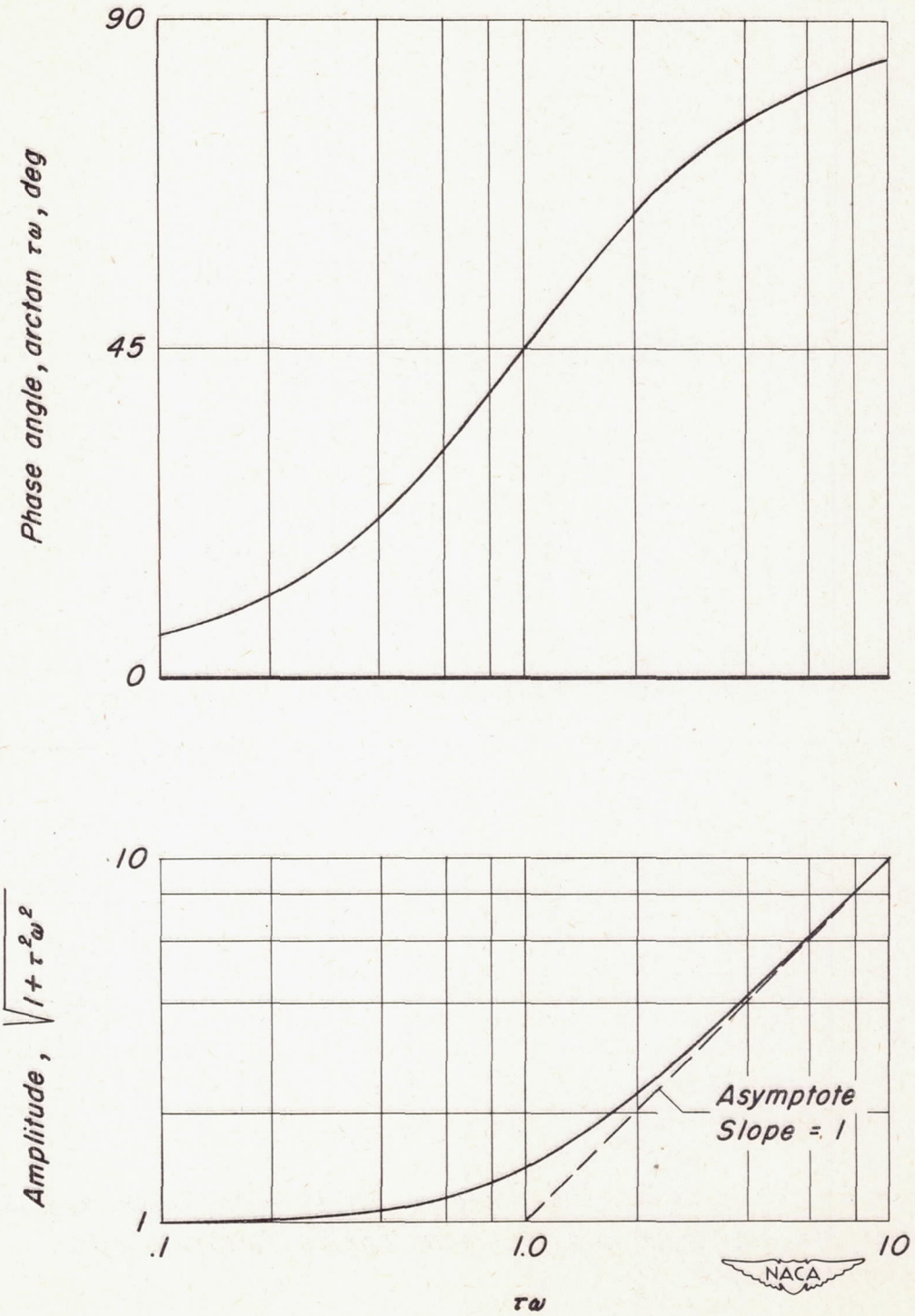

Figure 6.- Variation of the first-order term $(1+\tau i\omega)$ with nondimensional frequency $\tau\omega$.

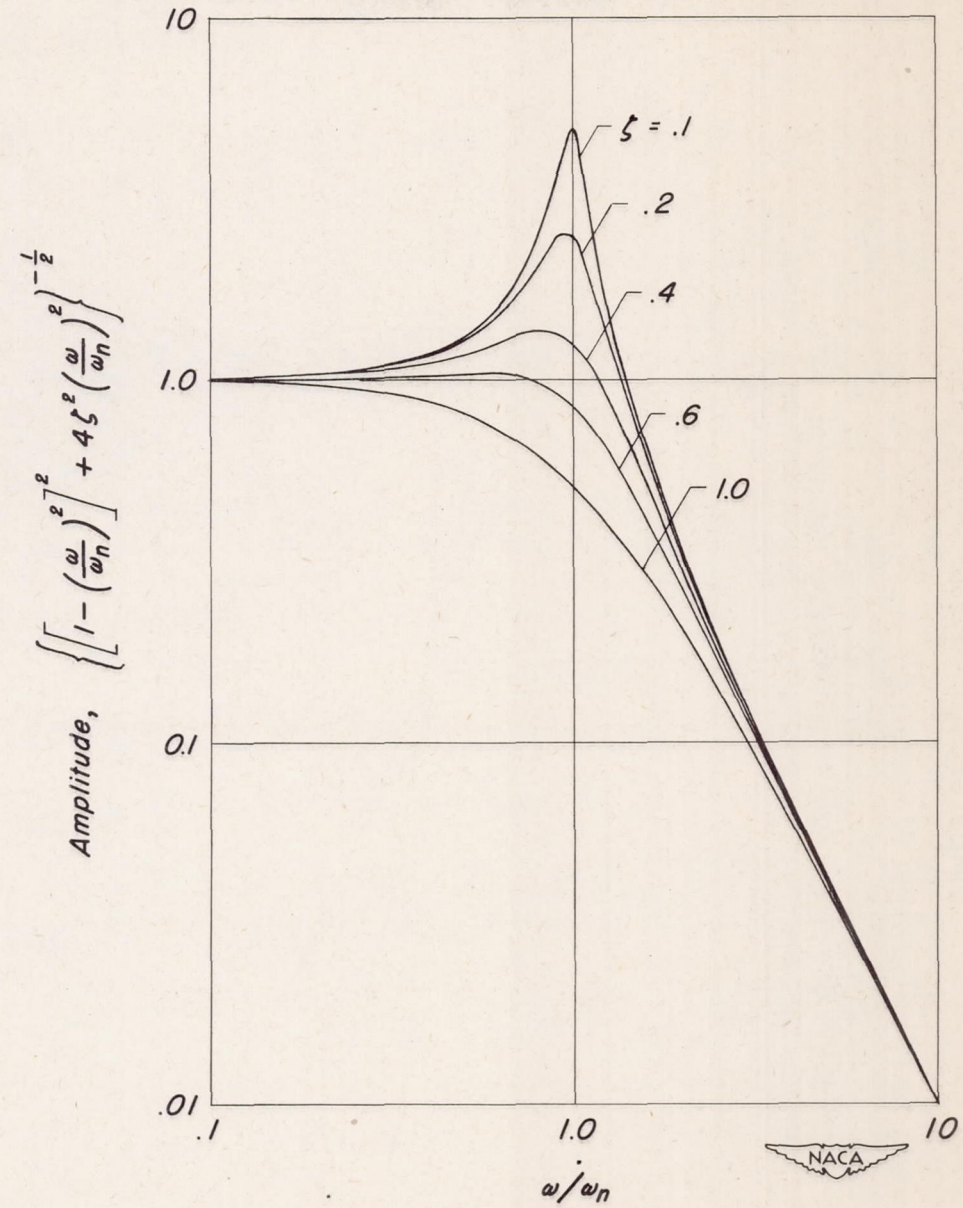

(a) Amplitude.

Figure 7.- The variation of the second-order term $\left[1+2\zeta\frac{i\omega}{\omega_n}+\left(\frac{i\omega}{\omega_n}\right)^2\right]^{-1}$ with nondimensional frequency $\frac{\omega}{\omega_n}$ for various values of damping ratio.

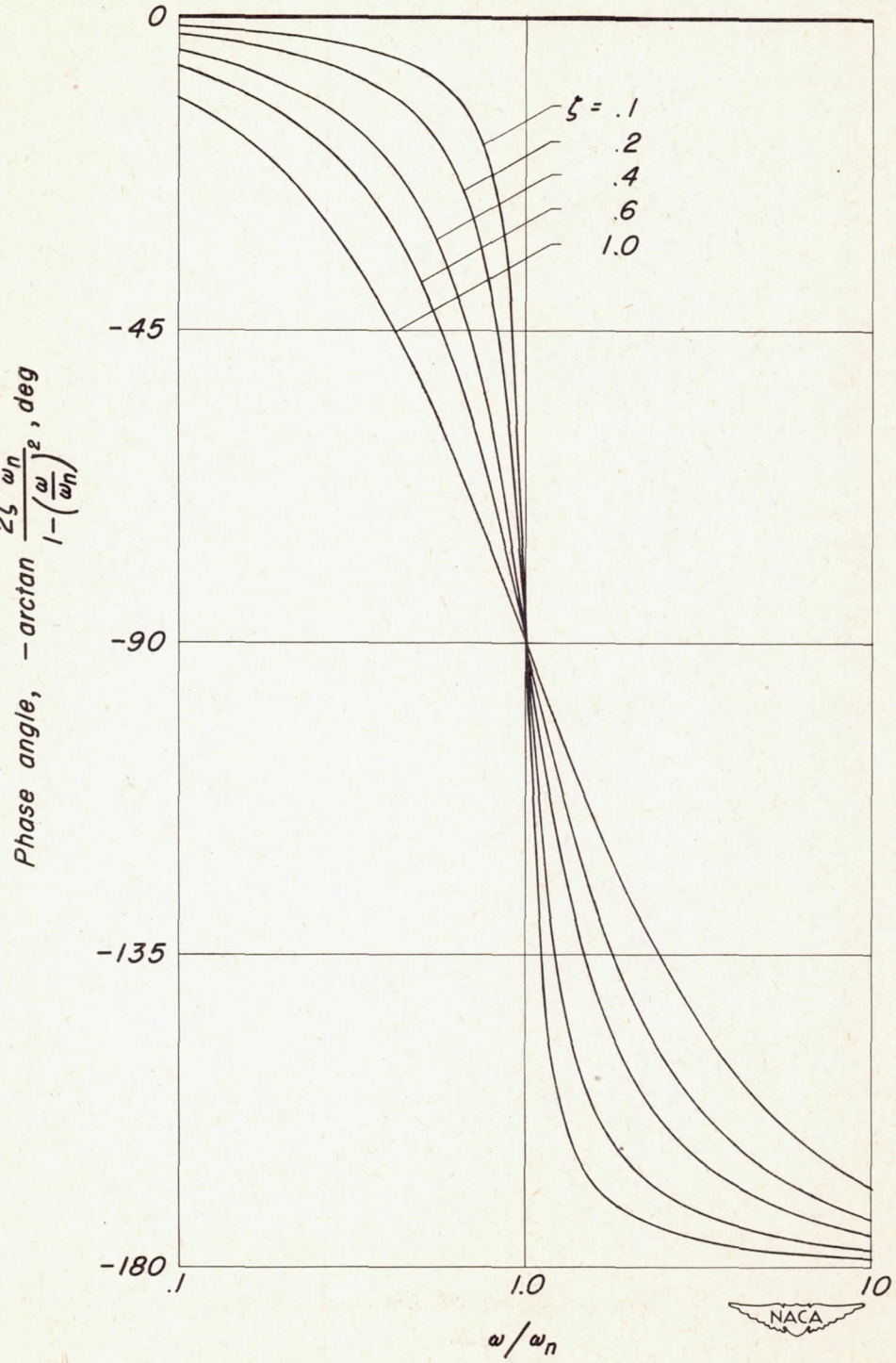

(b) Phase angle.

Figure 7.- Concluded.

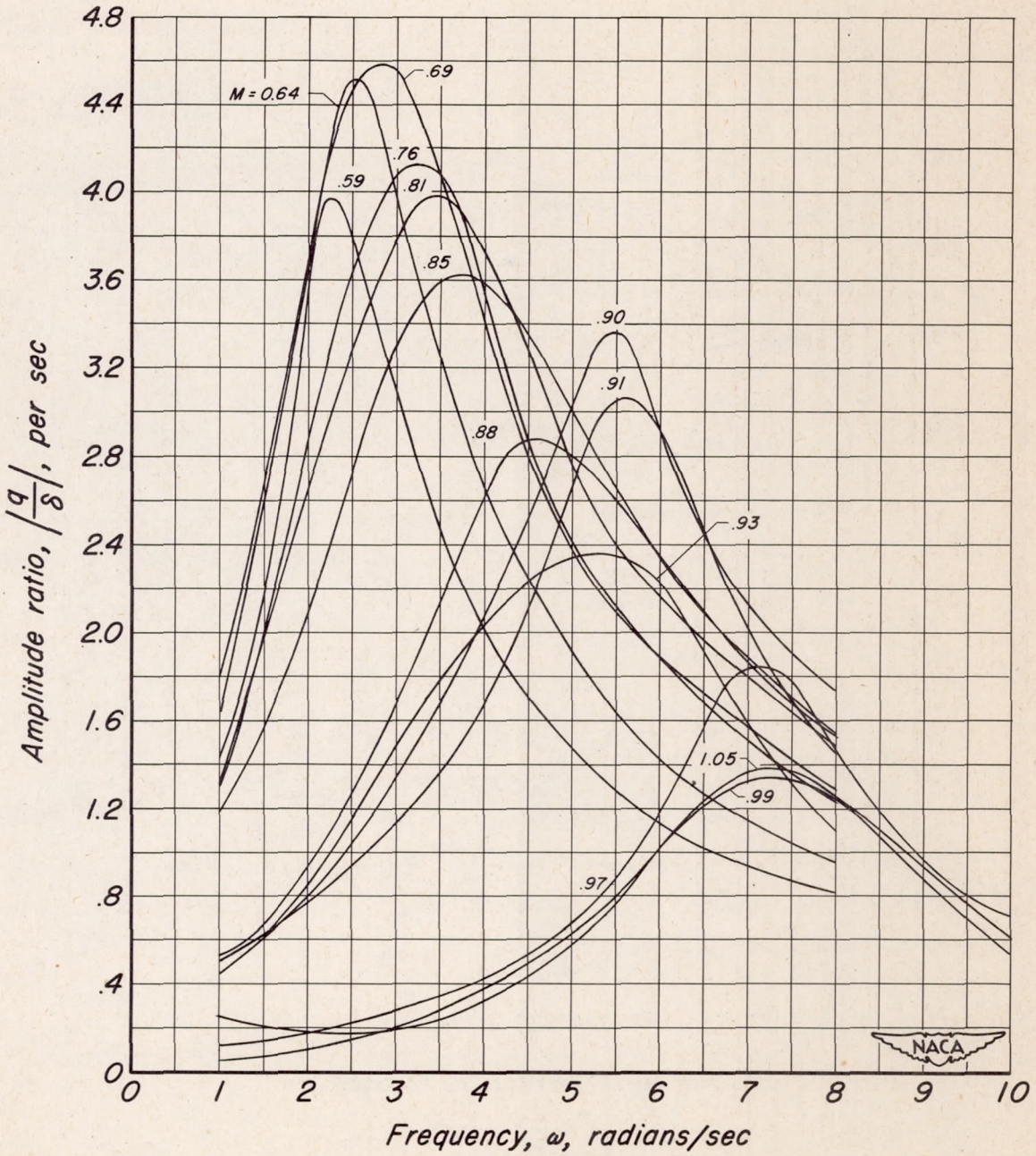

(a) Amplitude ratio versus frequency.

Figure 8. – Airplane pitching-velocity frequency response to elevator control inputs for various flight Mach numbers.

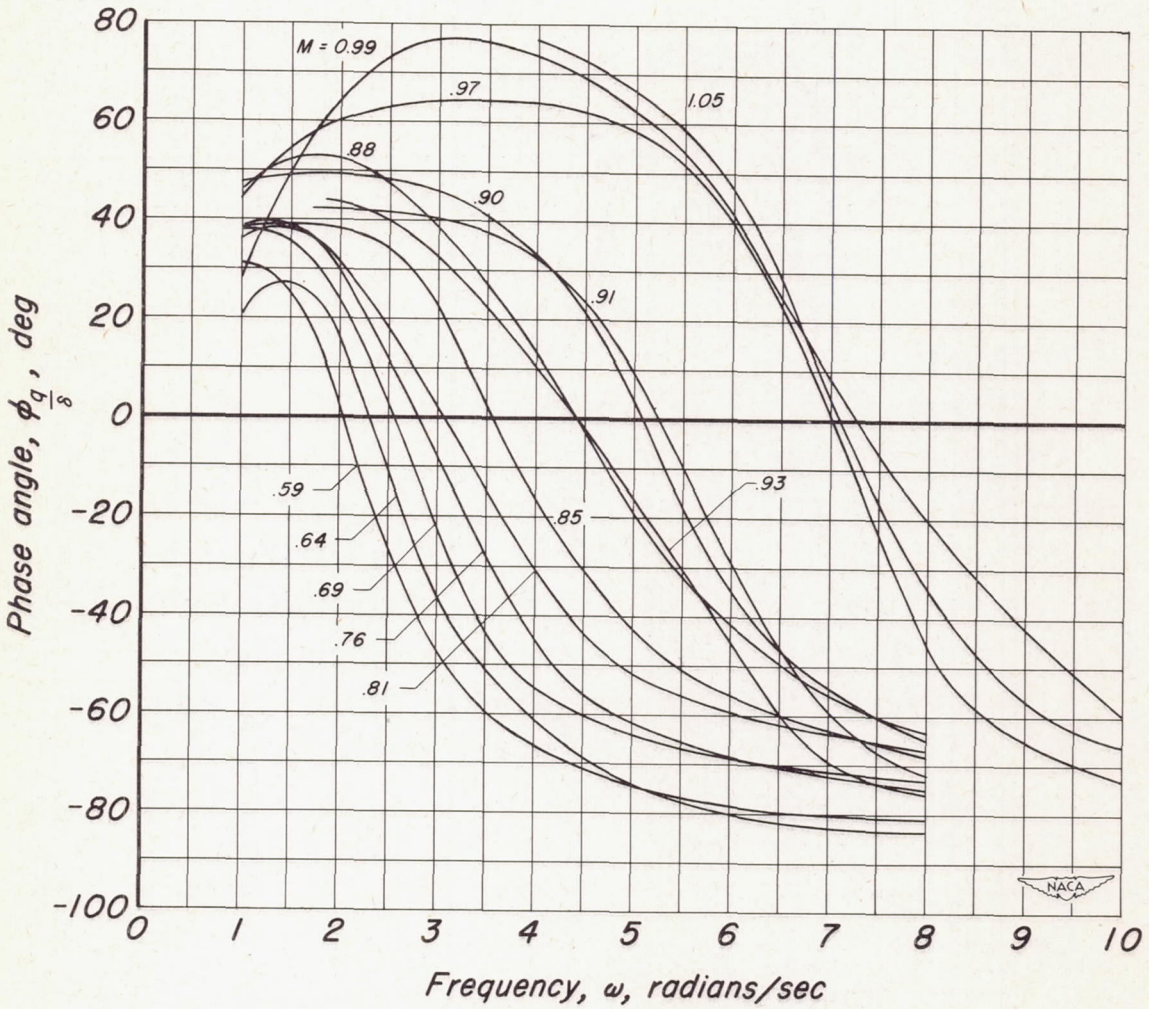

(b) Phase angle versus frequency.

Figure 8.- Concluded.

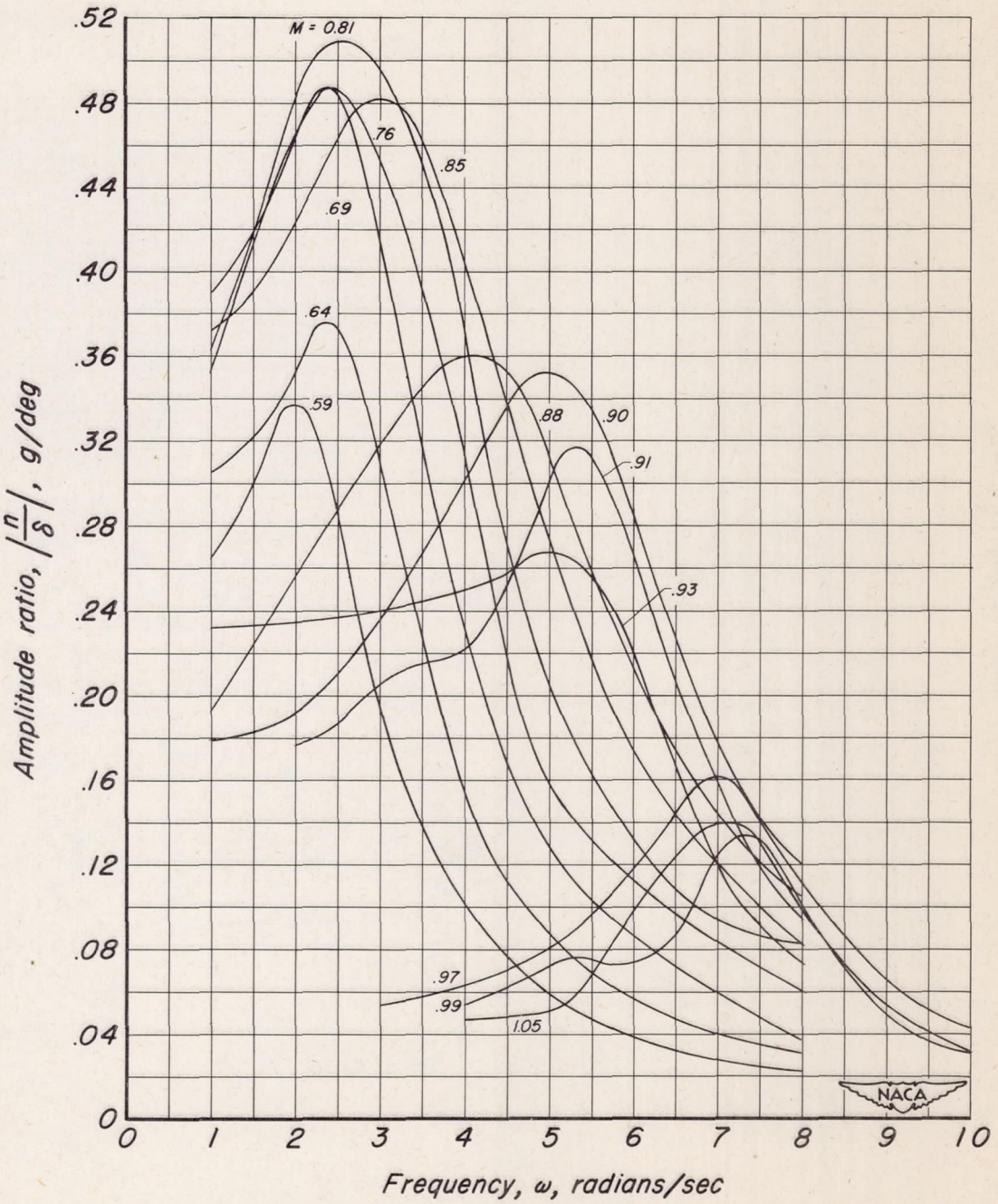

(a) Amplitude ratio versus frequency.

Figure 9.- Airplane normal-acceleration frequency response to elevator control inputs for various flight Mach numbers.

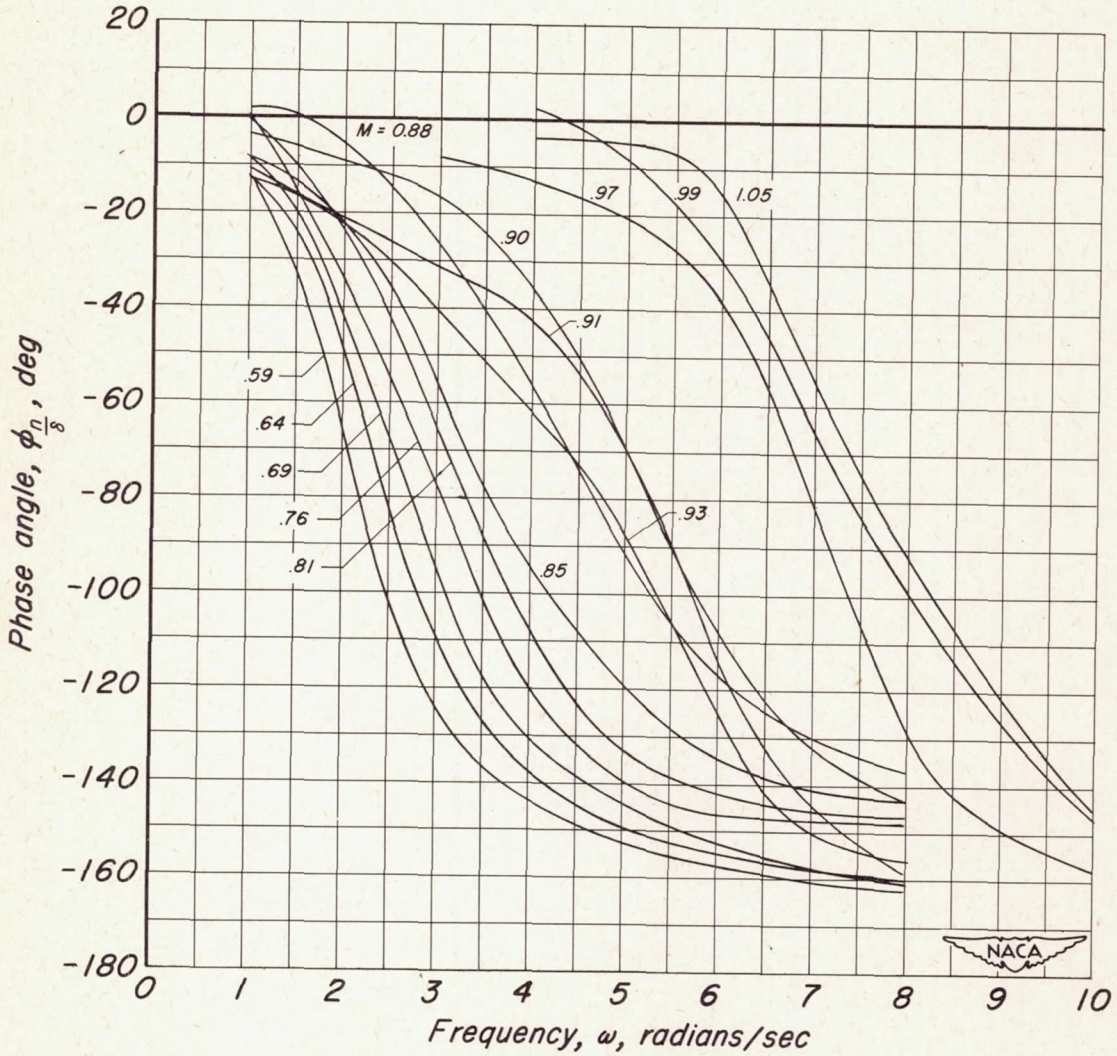

(b) Phase angle versus frequency.

Figure 9.- Concluded.

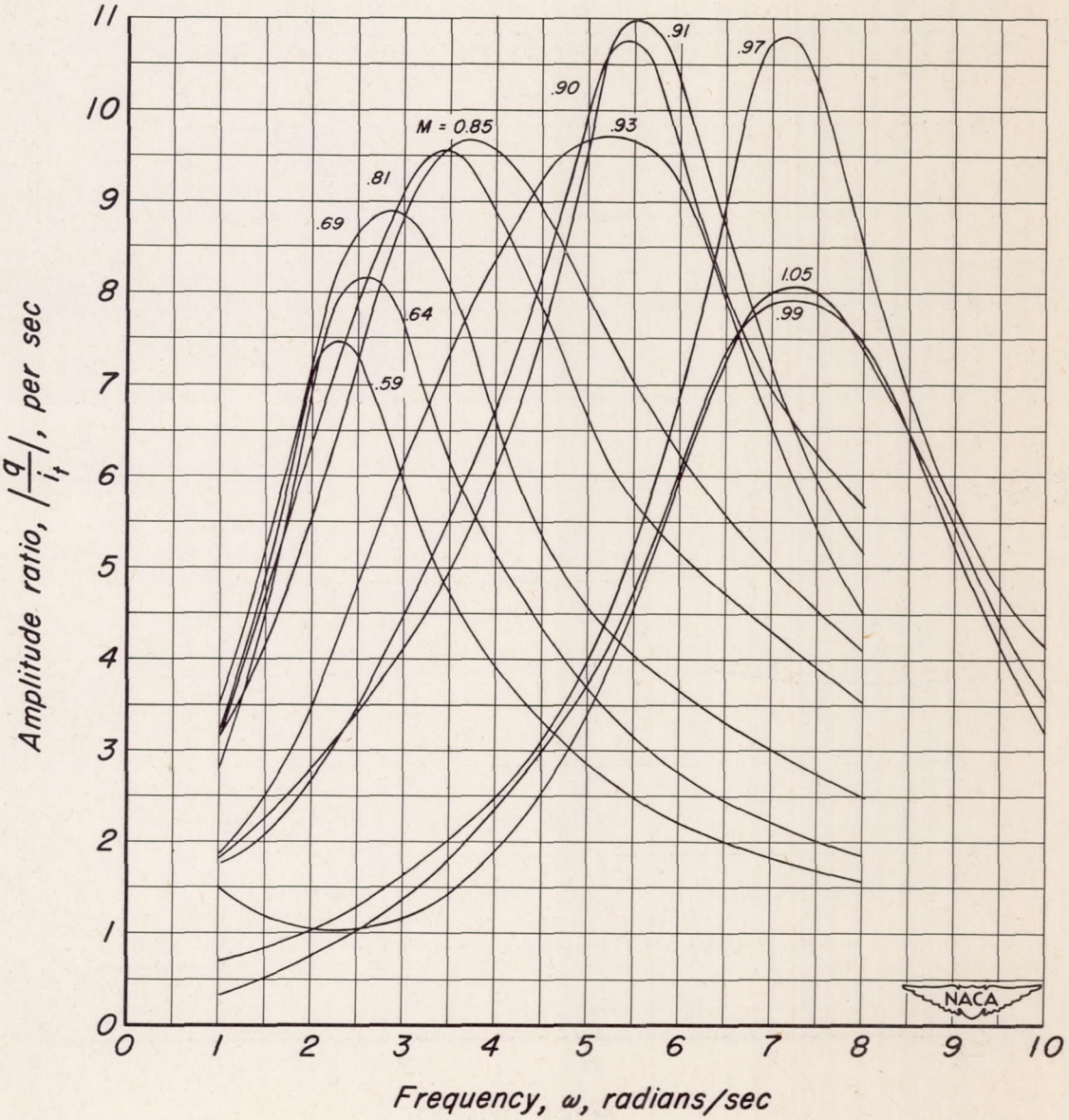

Figure 10.- Airplane pitching-velocity frequency response to stabilizer control inputs for various flight Mach numbers.

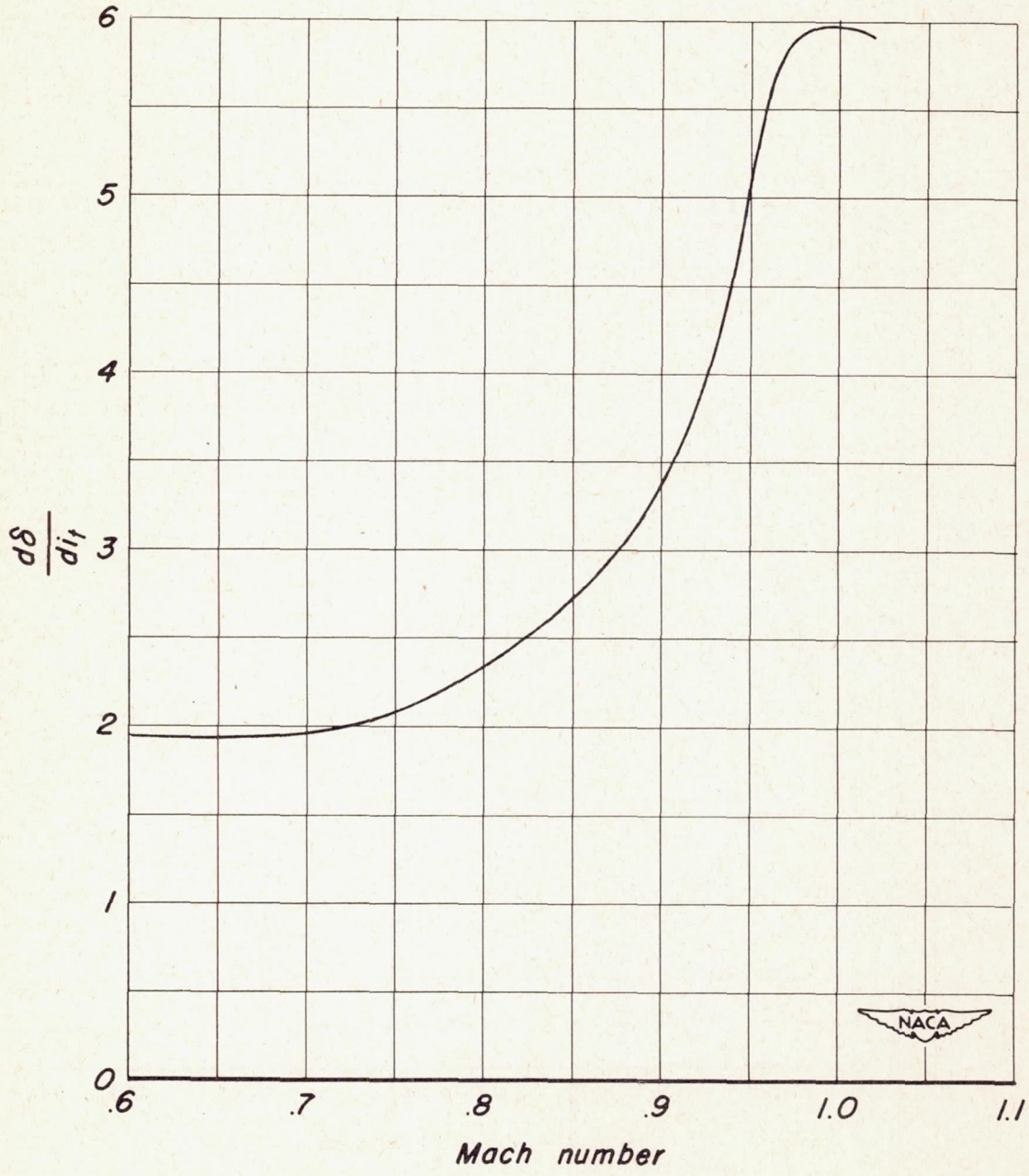

Figure 11.– Variation of the ratio of stabilzer to elevator effectiveness, $\frac{d\delta}{di_t}$, with Mach number.

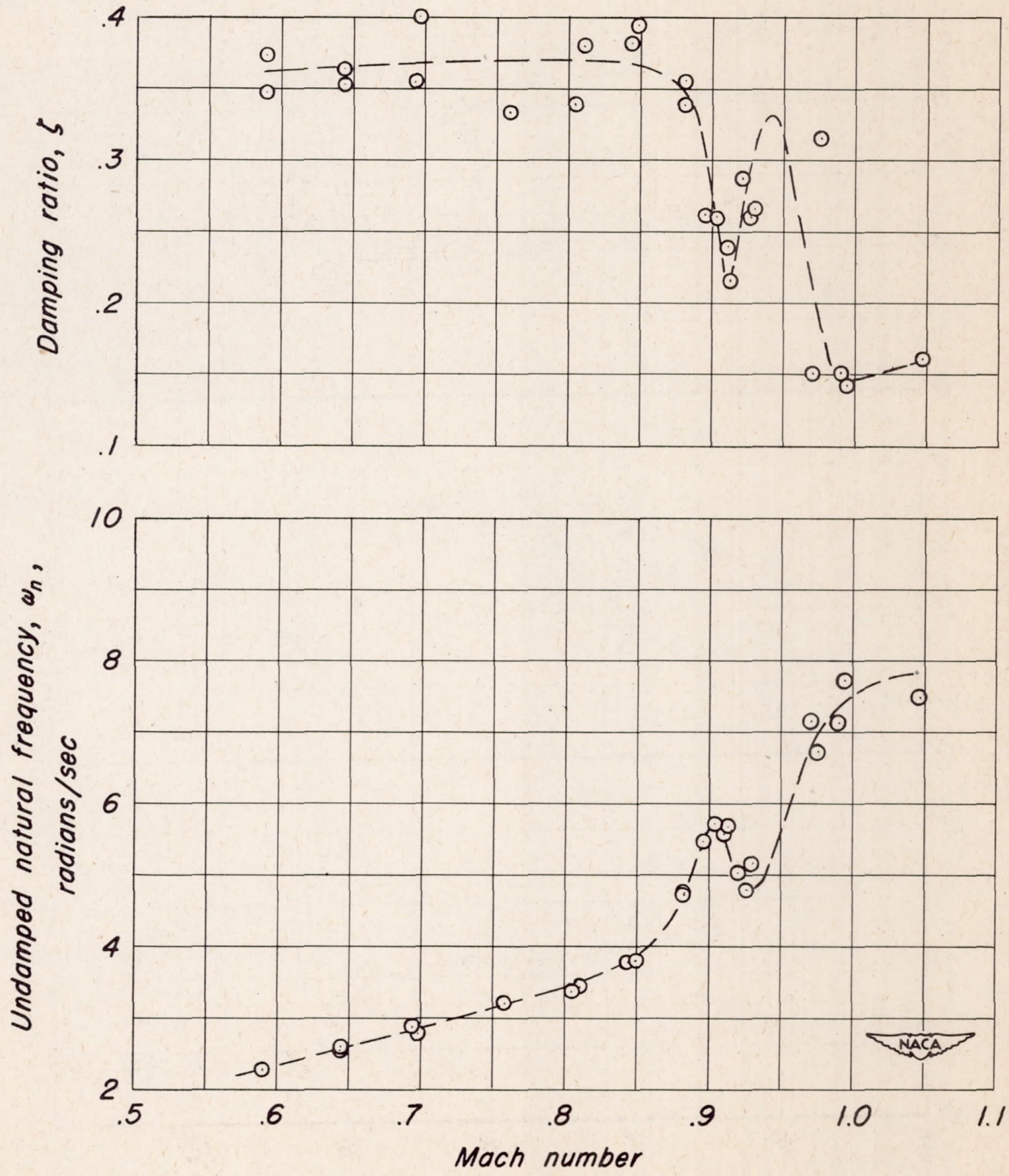

Figure 12.— Variation of damping ratio and undamped natural frequency with Mach number.

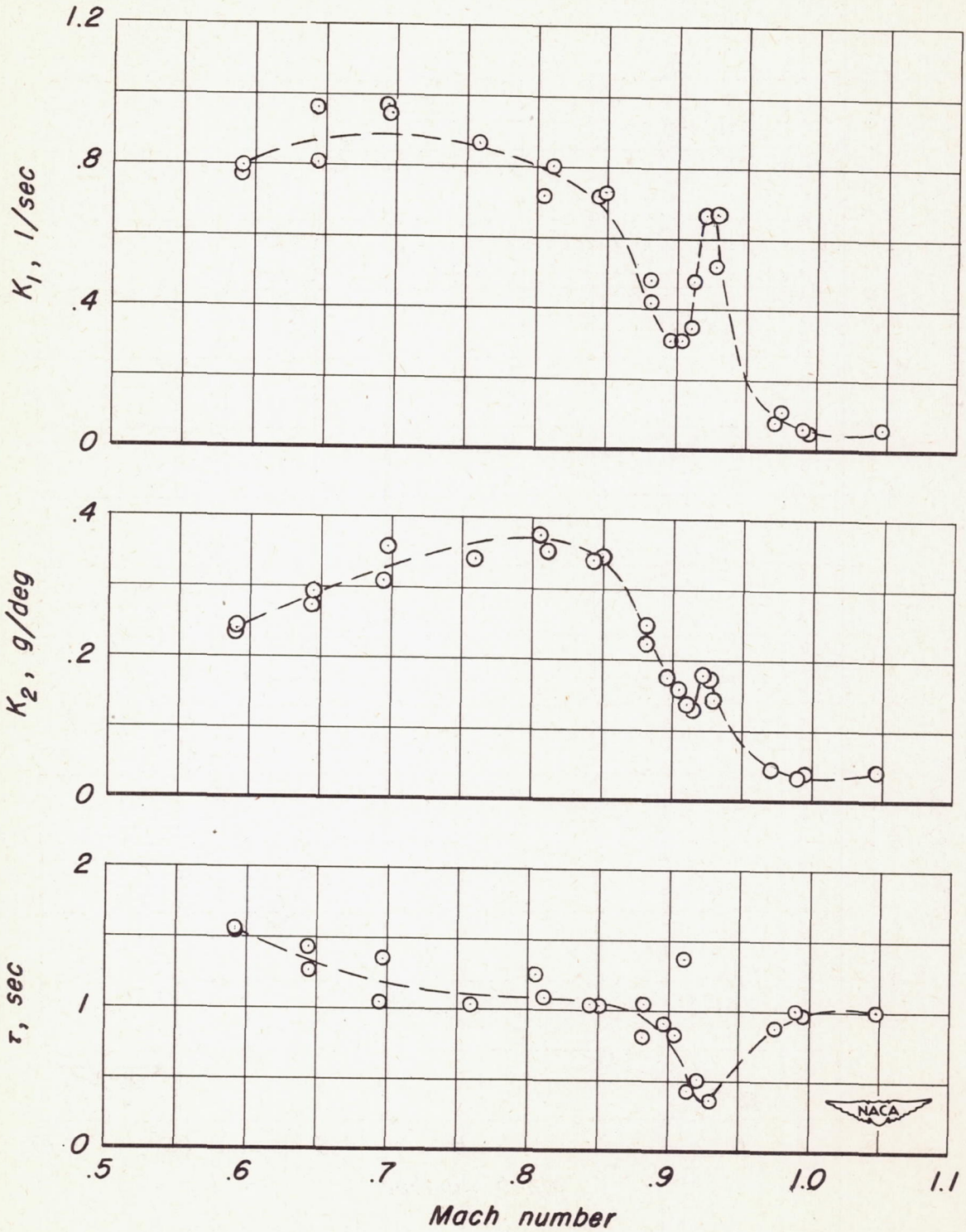

Figure 13.– Variation of the characteristic time, τ, and of the coefficients K_1 and K_2 with Mach number.

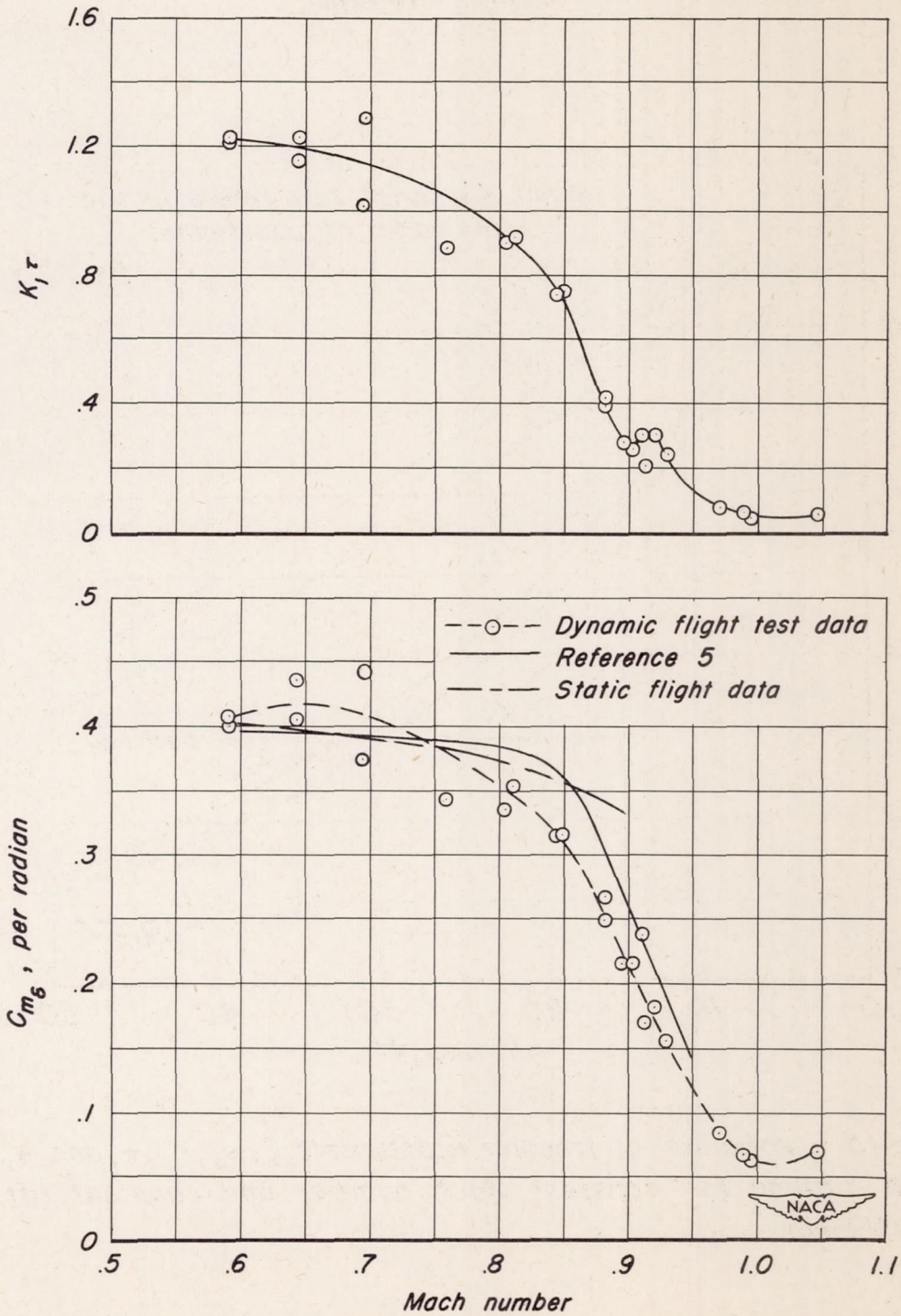

Figure 14.- Variation of the parameter $K_1\tau$ and elevator effectiveness C_{m_δ} with Mach number.

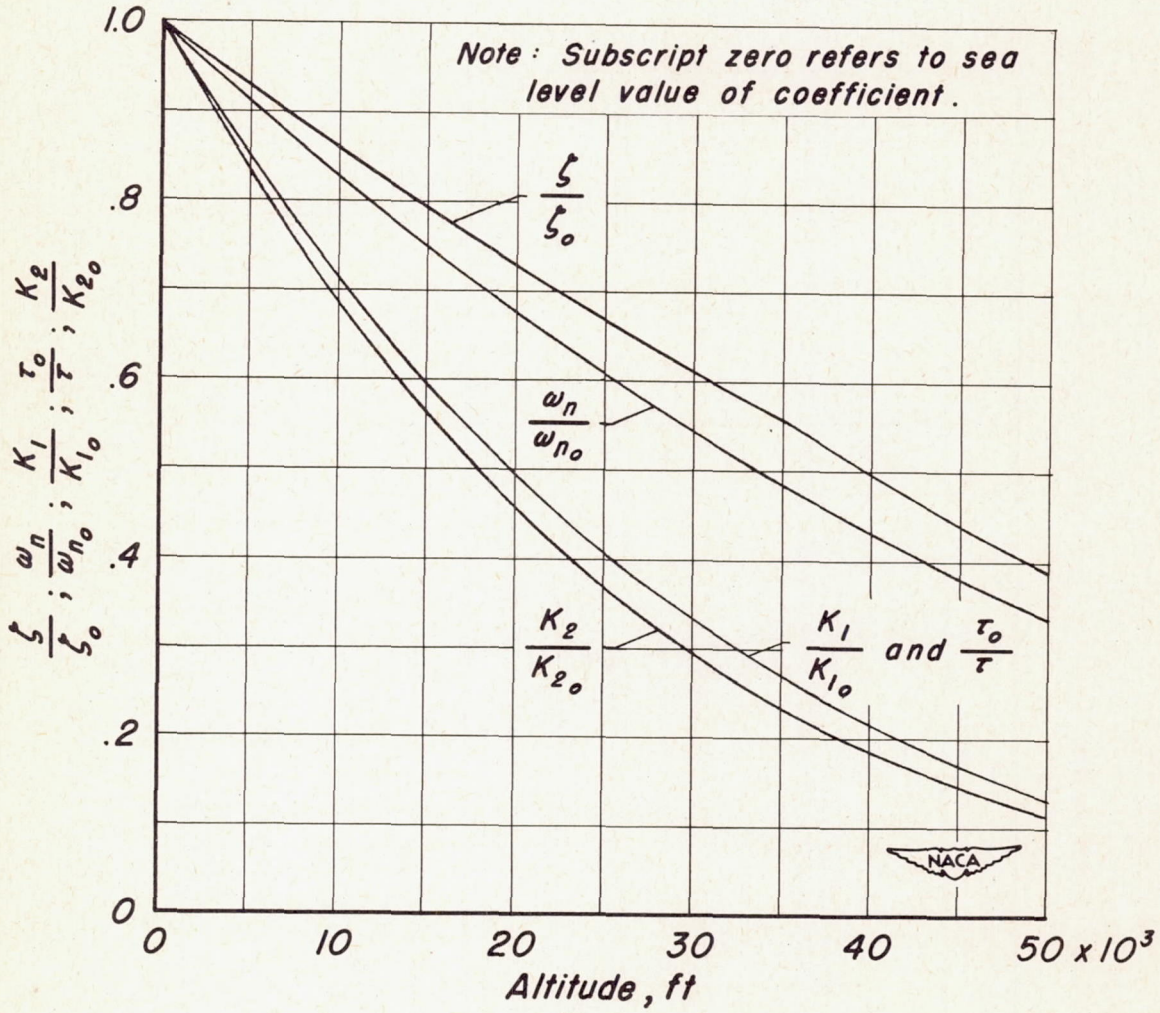

Figure 15.– Variation of transfer coefficients ζ, ω_n, K_1, τ, and K_2 with altitude for constant Mach number and constant lift coefficient.

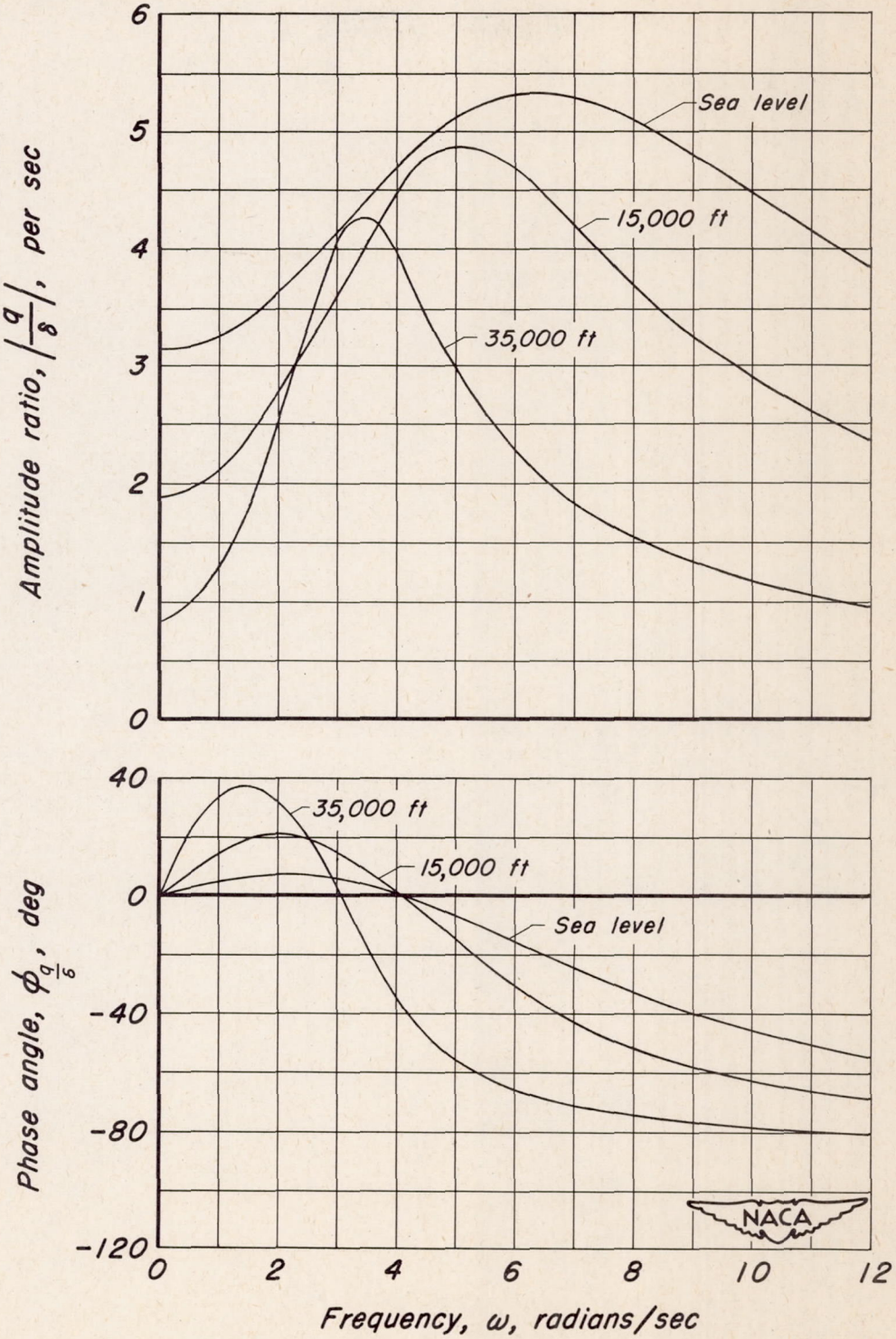

Figure 16.– Typical pitching-velocity frequency-response variation with altitude at Mach number of 0.81 .

NACA-Langley - 9-19-51 - 250